Università degli Studi di Genova

In collaborzione con

Libera Università di Brussel

Vrije Universiteit Brussel

FACOLTA' DI MEDICINA E CHIRURGIA

Master disordini muscolo scheletrici

FACULTY OF MEDICINE AND PHARMACOLOGY

Erasmus-program

In vitro 3D arthrokinematic analysis of coupled motion in the human upper-cervical spine during rotation high velocity thrust

Thesis presented as partial fulfilment of the Erasmus program of:

PROMOTER:

Prof. Dr. Erik Cattrysse

Academic year 2009-2010

In vitro 3D arthrokinematic analysis of coupled motion in the human upper-cervical spine during rotation high velocity thrust

Background:

Three dimensional analysis of coupled segmental motions in the cervical spine was only studied sparsely and in pure moment analysis. Only preliminary information exists on the kinematics of manual segmental mobilization. The present study focuses on the in vitro registration of upper cervical segmental coupled motions during manually performed therapeutic high velocity thrust techniques (HVT). The aim of the study was to collect qualitative information on the kinematics behavior of the upper-cervical spinal motion segments during applying manual therapeutic manipulation techniques. The information can help to understand the effect of manual therapy on spinal motion.

Methods and materials:

Twenty fresh human cervical specimens were studied in a test–retest situation with two examiners. Segmental kinematics HVT on C1-C2 were registered with a Zebris CMS20 ultrasound-based tracking system. The 3D aspects of motion coupling between main axial rotation and coupled lateral bending in C1-C2 and C0-C1 were analyzed by five parameters: the range of motion the three motion components, the cross-correlation and the ratio.

Results:

Prior a power analysis was performed: high power (0.957-0,995) and alpha error = 0.05 (xC1-C2, yC1-C2, zC1-C2) were found in the way to be more sure of the following tests.

The results indicate an inconsistent analysis reliability related to the not significant test of Spearman's correlation.

During HVT it can't find which is the major movement that occurs. Surely, there are clear high values in all movements (X,Y,Z) in C1-C2 (0,99-1,05 range) respect to C0-C1 (0,34-0,99 range). In rotation (Y) high values are evident both in C1-C2 than in C0-C1 as explained in the mean. Anyway, no difference among X,Y,Z in C1-C2 is present, while in C0-C1 the difference of rotation (Y), respect to X and Z, is very significant ($p<0,05$). The manipulation in rotation of C1- C2 involves a simultaneous non unintentional rotation (Y) in C0-C1 during the high velocity thrust.

***Conclusion*:**

The inconsistent analysis reliability is related to the not significant test of Spearman's correlation, maybe due a small mean with the large SD; in fact the results from the data are accurate but not precise.

The manipulation in rotation of C1-C2 doesn't distinguish which is the main movement that occurs in C1-C2 but it involves a simultaneous significant non unintentional rotation (Y) in C0-C1 during the high velocity thrust.

More work must be carried out in order to better analyze HVT techniques in the upper-cervical spines. The results of this in vitro study suggest that it might be important to examine kinematics of other manual techniques as they could have more segmental effects .

"I want to know how God created this world. I am not interested in this or that phenomenon, in the spectrum of this or that element. I want to know His thoughts; the rest are details…The most beautiful thing we can experience is the mysterious. It is the source of all true art and all science. He to whom this emotion is a stranger, who can no longer pause to wonder and stand rapt in awe, is as good as dead: his eyes are closed"

(A.Einstein)

<u>Acknowledgement</u>

"*Caro amico ti scrivo…*" (Lucio Dalla)

Thinking about notes of this song, and He knows why, I want to thank Prof. Dr Erik Cattrysse for the special trip that he gave me the opportunity to undertake.

His precious advises, endless patience and kindness have been a substantial support throughout my research. His professionalism and his enthusiasm let me realize what I want to do and how I want to get it. All this contributed to render me a *Sterke mevrouw*! Without your coffee break and your talks it would not has been the same thing.

Moreover I want to thank the "staff" of *Vrije Universiteit Brussel* for the hospitality demonstrated to me.

Thank you to *University of Genoa* for allowing me to do this experience, and to my Master teacher for enhancing my knowledge and improving my professionalism and broadening my mind. Sorry if sometimes I have stressed you with constant questions!

Thanks to my family because the family is the family: you are exceptional with me, always present, also far away. Without your advice, good words nothing would have been the same thing.

And finally many thanks to all my friends in the *Studentenhome* and fellow travelers of Brussels to teaching me English and making this period of my life special and unforgettable!

Silvia Gianola

Index

List of Abbreviation

A	Type I error, designated by the Greek letter alpha
ß	Type II error, designated by the Greek letter beta
CC	Cross-correlation coefficient
CS	Cervical spine
df	Degrees of freedom
FHA	Finite helical axis method
HA	Helical axis
HVLAT or HVT	High-velocity low-amplitude thrust
ISB	International Society of Biomechanics
PA	Posterior to anterior mobilization
KS	Kolmogorov-Smirnov test
X	Flexion-extension movement
Y	Axial rotation movement
Z	Lateral bending movement
ROM	Range of motion
ROM Z	Range of motion of coupled flexion-extension movement
ROM Y	Range of motion of the main axial rotation movement
ROM X	Range of motion of the coupled lateral bending movement
r	Retest
SD	Standard deviation
SMT	Spinal manipulative therapy
SF	Sinovial fluid
SPSS	Statistical Package for the Social Science version 14.0
t	Test
UCS	Upper cervical spine
Zebris CMS20	Ultrasound-based motion analysis device (Zebris Medizintechnik Gmbh Isny, Germany)
X-axis	From the anterior centre of the corpus perpendicular to the X-axis: segmental lateral bending axis.
Y-axis	Perpendicular to the X and Y axes: segmental axial rotation

	axis.
Z-axis	From right to left transverse process: segmental flexion–extension axis.
3D	Three dimensional
2D	Two dimensional
$0_2, 0_1, 0_0$	Finite helical angles

List of tables

List of figures

Fig ad1-6: angles α_x and ϑ_x

Fig ad3-1:flexion-extension r2-t2 C1-C2 in the Bland Altman plot

Fig ad3-3: lateral bending t1-r1 C1-C2 in the Bland Altman plot

Fig ad3-4a: correlation t1-t2 C1-C2 in the Bland Altman plot

Fig ad3-4b: correlation r1-t1 C1-C2 in the Bland Altman plot

Fig ad3-5: ratio r1-r2 C1-C2 in the Bland Altman plot

Fig ad3-6: flexion-extension r2-r1 C0-C1 in the Bland Altman plot

Fig ad3-7a: axial rotation r1-r2 C0-C1 in the Bland Altman plot

Fig ad3-7b: axial rotation t1-r2 C0-C1 in the Bland Altman plot

Fig ad5-1a: Bland Altman plot in X-Y C0-C1

Fig ad5-1b: Bland Altman plot in Z-Y C0-C1

1. Literature study

1.1 Introduction

Neck problem are very common in western population. Together with pain, a common feature of neck disorders is reduced cervical range of motion and reduced of joint position sense [1].

Spinal manual therapy techniques are commonly used in the management of musculoskeletal disorder of spinal origin. Several common conservative treatment are reported in the literature but the evidence is generally lacking, limited or conflicting [2].

In the first part of this thesis the aim is to make a review on the state of the art of a systematic literature research on joint movements produced by manual interventions at the cervical spine.

Therefore it's necessary to known physical characteristics of cervical spine but also the motion characteristics of non-linearity and coupling pattern of movement.

In the past segmental motion analysis of the cervical spine has been mainly approached two dimensionally.

More recently, a number of 3 dimensional studies on the kinematics of motion coupling in the cervical spine have focused on the kinematics of regional motion coupling . Limited but important information on 3-dimensional segmental coupled motions of the cervical spine is derived from studies applying well-controlled, pure movements of force in an vitro laboratory set-up. Methodological problems are related to the 3D-registration, regional as well as segmental, 3D-analysis and 3D-representation, with each method exhibiting its specific limitations. Although an important number of publications have reported on the kinematics manual mobilizations and manipulations at the level of the peripheral joints and spine, only a relatively limited number of studies have been performed on joint movements produced by manual interventions at the cervical spine [1]. Especially there are few study regarding the kinematics during high velocity thrust in the high cervical spine. Very few studies have been performed on the kinematic effects of spinal manipulative therapy at the level of the cervical spine [3]. These authors have focused on the global range of motion of the cervical spine during high-velocity thrust techniques.

In the second part of this thesis, it shows an experimental study in vitro during manipulation of high cervical spine.

Primarily it presents a method for the objective description of patterns of coupled motions during high velocity thrust by quantification of kinematics parameters. In particularly it wants to focus on the three-dimensional movement of segmental kinematics components of C0-C1 and C1-C2. What are the specific 3D-kinematic components of manual induced movements during the manipulation? The goal is to find a trend of motion coupling patterns in both segmental level analyzed during the manipulation and then to compare their results. In this way, the intervention to one specific motion segment could land the desired effect.

Similarly Cattrysse et al had published a study about a description of patterns of coupled motions by quantification of kinematic parameters during manual movement [4]. It could be interesting to analyze in the future a different behavior of patterns of coupled motion in manipulation and in manual movement.

1.2 Literature Research

1.2.1 Strategy research

Pubmed and Web of science within Web of knowledge were used, to search articles related to three main fields: Cervical, Manual, and Arthrokinematics.

The initial search was performed with free terms in Pubmed and Web science. The keys words were are:

1) "cervical": *cervical zygapophysial, cervical zygapophysial joint , cervical intervertebral, cervical intervertebral, atlanto-cranial, atlanto-occipital joint, atlanto-occipital, atlanto-axial joint, atlanto-axial, cervical disc, upper cervical spine, cervical spine, neck, craniocervical junction, craniocervical, cervical.*

2) "manual": *osteopathic techniques ,osteopathic spinal manipulation, osteopathic manipulative treatment ,osteopathic manipulation, osteopathic manipulative, osteopathic treatment, osteopathic, osteopathy chiropractic, osteopathy manipulation, osteopathy treatment, osteopathy, chiropraxis, chiropractic manipulation, chiropractic treatment, chiropractic, manual technique, manual techniques, high velocity thrust, joint manipulation, manipulation, joint mobilisation, mobilisation, mobilization movement, joint mobilization, mobilization, manual treatment, manual therapy, manual*.

3) "arthrokinematics": *joint biomechanics, biomechanics, joint kinematics, kinematics, kinetics, motion, movement, movement registration, motion analysis registration, motion registration, movement analysis, motion analysis, arthrokinematics.*

Because there were too many results, a consecutive search was performed with mesh terms limited to humans, adults, in English, German and French in the last 10 years, excluding pediatrics and surgery fields.

1.2.2 Results research

1.2.2.1 Pubmed

2446 articles were retrieved with the free words. Using the mesh terms research it became clear that many terms aren't indexed in the Pubmed: among all keys words found early in the free research, 72 articles were retrieved, of which 42 are published in the last 10 years .

1.2.2.2 Web of science

495 articles were selected, and 224 articles remained with the use of the additional limitations.

1.2.2.3 Selection

Retrieved articles were checked for relevance based on the title and abstract. Full test of the selected papers were retrieved in digital version, paper copy or by IBL-request.

51 articles were selected from 266 articles of both research.

I found some articles about the posteroanterior mobilization, the assessment and palpation, the manipulation or methods of measuring kinematics movement during manipulation and mobilization and some review.

1.3 Functional Anatomy and descriptive Artrokinematics

The upper cervical spine (UCS) consists of three articulating bones, the skull (occipital condyles, C0), the atlas (C1) and the axis (C2). This complex seems to play a significant role in the global kinematics of the cervical spine to maintain the head in the upright posture or to compensate coupling motions that occur at lower cervical segments. It is usually accepted that cervical patterns of motion are conditioned by neuromuscular factors, passive soft tissue tension such as fascia and ligaments and articular surface conformity. In addition, head stabilization during daily tasks is related to postural control in order to stabilize visual referential for achieving specific tasks [5].

The range of motion in the cervical area is characterized by C0-C1 which generates most of the flexion extension, C1-C2 which generates most of the rotation; while the lower segments of the cervical spine are less involved in movements: the flexion-extension and sidebending components are still more represented than the component of rotation (fig 1).

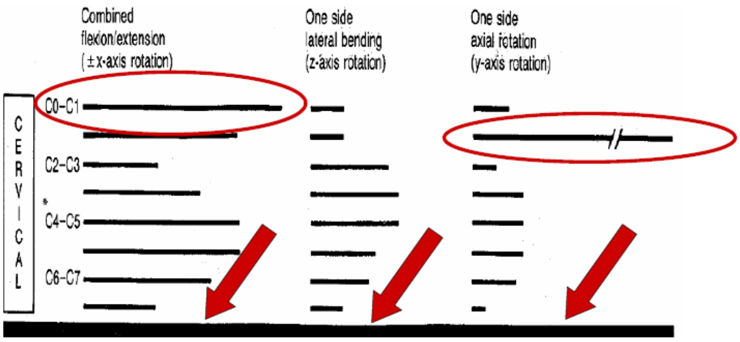

Fig 1. Range of movement in cervical spine

The stability of the atlanto-occipital joint stems largely from the depth of the atlantial sockets. The side walls of the sockets prevent the occiput from sliding sideways; the front and back walls prevent anterior and posterior gliding of the head, respectively. The only physiological movements possible at this joint are flexion and extension, i.e. nodding. These are possible because the atlantial sockets are concave whereas the occipital condyles are convex.

Flexion is achieved by the condyles rolling forwards and sliding backwards across the anterior walls of their sockets (fig. 2).

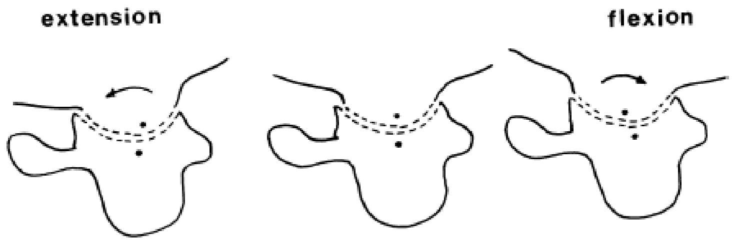

Fig 2. Right lateral views of flexion and extension of the atlanto-occipital joints. The centre figure depicts the occipital condyle resting in the atlantial socket in a neutral position. The dots are reference points. In flexion the head rotates forwards but the condyle also translates backwards, as indicated by the displacement of the references dot. A converse combination of movements occurs in extension. Nikolai Bogduk, Susan Mercer, Biomechanics of the cervical spine. I: Normal kinematics Clinical Biomechanics 15 (2000) 633±648 [6]

Axial rotation and lateral flexion are not physiological movements of the atlanto-occipital joints. They cannot be produced in isolation by the action of muscles. But they can be produced artificially by forcing the head into these directions while fixing the atlas. Axial rotation is prohibited by impaction of the contra lateral condyle against the anterior wall of its socket and simultaneously by impaction of the ipsilateral condyle against the posterior wall of its socket. For the head to rotate, the condyles must rise up their respective walls. Consequently, the occiput must separate from the atlas. This separation is resisted by tension in the capsules of the atlanto-occipital joints. As a result, the range of motion possible is severely limited. Lateral flexion is limited by similar mechanisms. For lateral flexion to occur the contra lateral condyle must lift out of its socket, which engages tension in the joint capsule [6].

The principal motion at the atlanto-axial joint is rotation and 40-70% of the total neck rotation occurs here. Rotation is initiated at the atlanto-axial joint and C1 rotation is complete before rotation of C2 and the lower cervical vertebrae begin. During rotation the ispilaterale mass of C1 rotates back into the spinal canal, thus narrowing it. Luckily, the spinal canal is at its widest at this level and anatomical studies have show that approximatelely 64° of right or left atlanto-axial rotation is required before there is sufficient narrowing to cause spinal cord compression [7].

In the neutral position the summit of the atlantial convexity rests on the convexity of the axial facet. As the atlas rotates, however, the ipsilateral atlantial facet slides down the posterior slope of its axial fact, and the contralateral atlantial facet slides down the anterior slope of its facet. As a result, during axial rotation the atlas descends, or nestles into the axis . Upon reversing the rotation the atlas rises back onto the summits of the facets. The restraints to axial rotation are the capsules of the lateral atlanto-axial joints and the alar ligaments. The capsules contribute to a minor degree; the crucial restraints are the alar ligaments. Dislocation of the atlas in rotation does not occur while so long as the alar ligaments remain intact. This feature further underscores the passive nature of the atlas, for the alar ligaments do not attach to the atlas; rather, they bind the head to the odontoid process of the axis. By limiting the range of motion of the head they secondarily limit the movement of the atlas [6].

1.4 Manipulation and mobilization

Manipulation and mobilization are two forms of manual therapy which are commonly applied to the vertebral column. The choice of which form of manual therapy to employ in any given situation may be dictated by a variety of considerations including the technical training and skill of the practitioner, and perceptions of risk versus benefit [8]. Reports and overviews of clinical studies involving manual therapy often fail to adequately distinguish between the two types of therapy in their descriptions of methods [9], and, when described, may fail to demonstrate a therapeutic advantage for one over the other [10].

Spinal manipulation has been defined as a high-velocity, low amplitude thrust applied to a bony prominence of a vertebral motion segment, whereas a mobilization is generally regarded as a lower-velocity movement which may be applied over a broader area. Relatively few studies have examined the biomechanics of the neck during manipulation and mobilization [11].

1.5 Manual mobilization: arthrokinematics analysis of upper cervical

The manual therapy technique used most often by physiotherapists when treating the neck and found in this research of literature is the posterior-to-anterior (PA) mobilization technique. The PA mobilization technique can be described as an oscillatory force applied to the spinous process (central PA) or articular (unilateral PA) processes of the spine.

Posterior to- anterior mobilizations to the cervical spine are usually applied with the pads of the thumbs, but occasionally, therapists use the heel of the hand [12]. Therapists select 1 of 4 grades, which have been described by Maitland et al [13] depending on the aim of treatment.

Other mobilization is segmental spinal mobilization that involves to one specific motion segment. A few of articles are reported in the literature. The three dimensional aspects of movements are described in terms of coupling between different motion components.

These associated motions are usually unintended and, in the upper cervical spine, they are described as occurring in a mainly contralateral coupling pattern during axial rotation. Associated or coupled motions, however, may also occur during so called planar flexion-extension mobilization [1].

1.6 Joint kinematics analysis

Arthrokinematics is the analysis of joint motion in terms of bone-embedded coordinate systems closely related to referred motions in the anatomical plane. More specifically, intra-articular kinematics evaluates joint motion using coordinate systems based on the configuration of the joint. In the last decade, the study of intra-articular kinematics has gained an orthopedic interest in the context of replacement or support of joints, a clinical and ergonomic interest in comparing normal movements with pathological movements and an interest in understanding specific manual therapeutic mobilization/manipulation techniques [14].

Three-dimensional (3D) joint kinematics analysis of the spine could supply information such as location and orientation of instantaneous axis of movement. Indeed, previous studies investigating cervical kinematics mainly used 2D analysis for describing joint displacement and motion axis location. Thus, changes in the orientation of the axis of rotation during motion were mostly lacking. Various studies have suggested 3D-methods using helical axis computation for analyzing joint kinematics such as for the knee, wrist, foot and lower cervical spine. In this way, results clearly document that the helical axis (HA) provides extended data concerning segmental coupled motion during global movement [5].

To fully describe 3D-motion of a rigid body, six independent measure are required. These six degrees of freedom are defining three rotational and three translational movements around and along the axes of a generally orthogonal reference frame. In clinical analysis, there is an interest to depict 3D joint and segment angular displacement in terms of three meaningful and independent quantifiers, representing the three rotational movements components, which, from a functional anatomical point of view, denote respectively flexion/extension, ab-/adduction, and endo/exorotation [1].

The helical axis of motion is as alternative to the three rotations and three translations description of intervertebral motion. Using the helical axis of rotation, the motion is described by the position and direction of an axis of motion, together with a scalar translation along this axis and a scalar rotation around it. Thereby, the finite Helical Axis (FHA) analysis has been preferred as a valid approach to obtain a functional representation of a joint movement. This axis can be considered as the 3D equivalent of the finite centre of rotation in a 2D analysis motion and is defined by its orientations, its position, the shift along and rotation about the axis . However, even though the FHA is useful for the representation of 3D joint kinematics, this approach may cause interpretational problems among clinicians. So that it has been replaced with the use of the finite helical angles, a mathematical derivate decomposition of the rotation around the FHA according to the X-axis, Y-axis, and Z-axis of the defined bone embedded coordinate system. The calculation of the finite Helical Angles showed to be appropriate for analyzing coupled rotations. The rotation vector n0 (x,y,z) was decomposed in three components corresponding to the helical angles 0_2,0_1,0_0. In this way the movement of a motion segment, represent by an angle o around a FHA with a direction vector n, could be described as a rotation by these helical angles 0_2,0_1,0_0 simultaneously around three orthogonal axes Z, Y and X, respectively. The helical angle approach offers some important advantages over other methods. It's not sequence dependant as the Euler-Carden s and the possibility of comparing angle analysis techniques and compared to the FHA representation, it gives an easier interpretation of individual motion coupling patterns and possibility of comparing group descriptive statistics [1].

The 3D aspects of movements are described in terms of coupling between different motion components. Coupling pattern between axial rotation and lateral bending are generally described as ispilateral or controlateral.

1.7 Coupling movement

Coupled spinal motion is the rotation or translation of a vertebral body about or along one axis that is consistently associated with the main rotation or translation about another axis. During movement, translation occurs when all elements within that segment move in the same direction with the same velocity. With movement, rotation occurs as a spinning or angular displacement of the vertebral body around some axis. Biomechanical coupling is 3-dimensional (3D), takes place within 6 df, and is often described using the Cartesian coordinate system. The 6 df can translate along and rotate about each orthogonal axis. The 3D motions in humans correspond to flexion/extension, rotation, and side-bending forces; one specific movement initiation (such as sidebending) theoretically activates movement in the other 5 component motions. The behavior of the coupled pattern is dependent on the first motion of initiation (eg, sidebending),the posture of the spine, and the pathology of the segment. Coupling of the cervical spine is of importance to manual clinicians during assessment of pathology [15] and treatment application. In theory, measurements of coupling motion are useful to diagnose pathologic disorders such as clinical instability due to degeneration, disease, or trauma [16].

Many manual medicine disciplines base specific mobilization, manipulation, and muscle energy techniques on selected theories of coupling direction. Common to these manual medicine treatment techniques is a concept called apposition. Apposition is a close packed combined movement and is, in essence, the biomechanical opposite of a coupled movement. This close packed movement is often preselected, based on the theoretical preexisting direction of coupled motion. Apposition movements are frequently used during manipulative procedures and are termed in osteopathic literature as a locked position. Ironically, treatment methods that are based on coupling theories are often inconsistently reported and are generally defined through “expert-based” learning models [15].

Coupled motion patterning of the cervical spine has been based on a regional approach in previous research. Segmental motion analysis of the cervical spine has been mainly approached two dimensionally. Limited information on 3D coupling between the cervical segments has been derived from controlled studies applying pure moments of forces, meaning that controlled forces are applied at fixed distances in specific directions according to a predefined local reference system [17-18-19]. Panjabi et all [19] has reported combined movements in the upper cervical spine in different positions, applying pure moments of force. These authors registered the largest angular displacements in the axial rotation component and found them to be contralaterally coupled with lateral bending in the atlo-axial joint.

In a systematic review of literature Cook [15] et al investigate the evidence of consistency of reported directional coupling patterns among selected studies. According to Cook in the assessment of 3D analyses, all investigators reported that side flexion and rotation occur to the same side during side flexion or rotation initiation at the cervical segments of C2-3 and caudal. Consistency was observed in the upper cervical segments (C0-1, C1-2) during rotation initiation, where the segments exhibit side flexion motion to the opposite side. However, C0-1 and C1-2 show less consistency across studies during side flexion initiation. There may be several reasons for this coupling variability: anatomical variation, structure, and mechanical influences, the differences associated with in vitro and in vivo specimens, the instrument used during the measurement process may lead to variable results [15]. Furthermore, Panjabi et al [16] reported that upper cervical spine posture does affect coupling amount and direction, and because the degree of postural change that does effect coupling direction has not been verified, the ability to standardize a position has not yet been verified.

In according to Cattrysse et al [1] several authors have reported ranges between 45°-88,5° for the active axial rotation at the C1-C2 motion segment from in vivo studies using stereo-photogrammetric techniques. In an vitro study Cattrysse et all reported the mean range of axial rotation motion is situated in the lower range of the values emanating from the in vivo studies. This coupled lateral bending reached almost half of the mean axial rotation motion at the atlo-axial level in the contralateral coupling group, and was slightly smaller in the specimens presenting ipsilateral coupling pattern[1].

The use of cross-correlation analysis coefficient showed to be a more useful and objective tool to analyze patterns of coupled motion, especially when the patterns are less clear to analyze like in the lateral bending mobilization of the atlanto-axial joint.

The coupling pattern of axial rotation and contra-lateral lateral bending reported in the atlanto-axial joint in a pure moment laboratory set-up was also observed in most specimens in this in vitro analysis of manual planar mobilization. The contra-lateral coupling pattern also seemed to be dominant in less controlled situations mimicking mobilizing techniques. It seems fair to expect it also to be present in clinical practice [20].

1.8 Manipulation: arthrokinematics analysis of upper cervical

Spinal manipulative therapy (SMT) is commonly performed in osteopathy, chiropractic and in related fields as manual medicine or manual therapy. A manipulation consists in a thrusting, impulse-like force applied to a specific vertebra or to a region of several vertebrae [3]. Hypotheses on mechanism of action for the effect of manipulation focus on resolution of altered body segment kinematics and distribution of loads between joint tissue components [21].

There have been many attempts to explain the physiology of the various effects of spinal manipulation, particularly those of the high-velocity low-amplitude thrust (HVLAT or HVT) type. As its name suggests, this type of manipulation uses a high velocity "impulse" or "thrust" which is applied to a diarthrodial synovial joint over a very short amplitude. This type of manipulation is usually associated with an audible "crack," which is often viewed as signifying a successful manipulation. The cracking sound is considered to be caused by an event termed "cavitation," occurring within the synovial fluid (SF) of the joint (fig 3). Cavitation is the term used to describe the formation and activity of bubbles (or cavities) within fluid through local reduction in pressure [22].

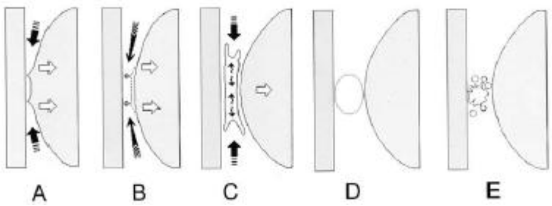

Fig 3. Cavitation. Schematic representation of surface geometry and shapes of growing cavities at a high separation speed (v >> vc as is likely with HVLAT manipulation) where doughnut (toroidal)-shaped cavities form around, rather than at the center, of the contact zone. **A,** During separation, the outer regions of the circular contact zone become pointed. This deformation occurs because at this speed, the central region of the contact zone separates, whereas the outer region remains almost unmoved, creating a circular rim. **B,** Surfaces snap back at the circular rim where the cavity initially forms. **C,** Coalescence of toroid into single dendritic cavity that grows to reach a maximum bubble size. **D,** The newly formed spherical bubble reaches its maximum size. **E,** Because of its instability, the single bubble collapses to form a "cloud" of many smaller bubbles (demonstrable by radiography as a radiolucent region), which later shrink as the gas and vapor dissolve Adapted from Chen YL, Kuhl T, Israelachvili J. Mechanism of cavitation damage in thin liquid films: collapse damage vs. inception damage. Wear 1992;153:31-51. [22]

Commento [lvE1]: Be sure to include these references in your own literature list en refer to the publication where you took this picture from

Very few studies have examined the kinematics of spinal manipulative therapy. Some authors have focused on the global range of motion of the cervical spine during high-velocity thrust techniques [3] while others have analyzed forces transmitted to the lumbar vertebra during lumbo-sacral manipulation [23].

One of the more difficult segments to manipulate with safety and comfort is C1–2. At this spinal level, it is imperative to seek end range by use of the coupled movements of side bending and rotation. Take, for example, a loss of rotation to the right due to dysfunction at the left C1–2 facet. To perform HVT to the left C1–2, contact must be on the left C1–2 facet. The therapist's left index finger is placed on the arch of the atlas and the right forearm supports the occiput (fig. 4). The occiput is side bent to the left, which effects right rotation at C1–2. This is followed by further rotation of the C1–2 joint until the end range for that segment is determined. This should be approximately half of the normal available physiological cervical rotation. The thrust is given via the left hand in an upslope direction towards the lower aspect of the right orbit and there is no added occipital rotation (Fig. 4). This procedure ensures that rotation at the C1–2 joint is still achieved, but the amount of physiological rotation is reduced. Again, the amount of force used is 80% with the left contact hand and 20% with the support hand and forearm. Importantly, as with the previous C0–1 technique described, the support hand is more of a counter pressure rather than an assistor [24].

Commento [IvE2]: Refere to the original text where this part comes from

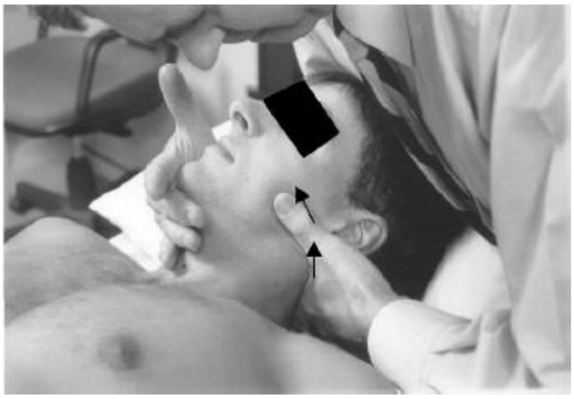

Fig 4. Direct HVT of C1–2. Upslope or rotation technique to the right (arrow indicates direction of thrust). W. A. Hing, D. A. Reid, M. Monaghanw. Manipulation of the cervical spine. Manual Therapy (2003) 8(1), 2–9 [24]

Three dimensional analysis of coupled segmental motions in the cervical spine was only studied sparsely and in pure moment analysis. Only preliminary information exists on the kinematics of manual segmental mobilization.

The aim of the study of Cattrysse et al [25] was to collect qualitative information on the kinematics behavior of the upper-cervical spinal motion segments during planar induced movements and while applying manual therapeutic manipulation techniques. The information can help to understand the effect of manual therapy on spinal motion. During HVT traction on the C0-C1 level the thrust results in a 3-dimensional translation. The main direction is lateral, coupled with a smaller axial and sagittal displacement. The rotational HVT on the level C1-C2 results in an additional axial rotation component of approximately 2°, with almost no rotational components in flexion-extension or lateral bending directions. This axial rotation component is however again accompanied by translational displacements in all three directions. The largest translation takes place in the lateral direction. These results show that manual induced segmental coupled movements in the upper cervical spine can be analyzed in vitro by means of an electromagnetic tracking device. The largest motion at the atlanto-occipital level is flexion-extension as is described in literature, while at the atlanto-axial level the rotation is the motion whit the largest amplitude. HVT-techniques can induce axial translational displacements and additional axial rotation in traction and rotation techniques respectively.

2. Experimental Study

2.1 Introduction

Very few studies have examined the kinematics of spinal manipulative therapy. Some authors have focused on the global range of motion of the cervical spine during high-velocity thrust techniques [3] or on lower cervical spine [26, 27] while others have analyzed forces transmitted to the lumbar vertebra during lumbo-sacral manipulation.

Therefore, the reproducibility of the 3D-kinematic aspects of motion coupling pattern of segmental manipulations is not yet known. The detection of a dysfunctional spinal segment seems to be achievable with good agreement between repeated measurement and between examiners. Reproducibility of segmental 3D-aspects of manual mobilization of the atlanto-axial joint in an *in vitro* situation can differ between examiners. The results of a recent study indicate a possible tendency to higher reproducibility if mobilizations are performed by an examiner with high experience, expertise and a high level of familiarization in applying the specific techniques [28].

2.2 Purpose

Very few studies have examined the kinematics of spinal manipulative therapy. So far, a large number of studies using in *vitro* and *in vivo* set-ups have been able to investigate just the normal cervical moving patterns. In the present study an *in vitro* analysis on twenty fresh human spinal specimens in a test-retest situation with two therapists is presented.

The results derived from the combination of using a ultrasound device for continuous motion registration with manual mobilization techniques are reported and compared with other previous *in vitro* studies on embalmed specimens [28].

The present study focuses on the *in vitro* registration of upper cervical segmental coupled motions during high velocity thrust techniques. The aim of the study was to collect quantitative information on the kinematics behavior and motion coupling patterns between axial rotation and lateral bending at the atlanto-axial motion segment during high velocity thrust techniques. Such information can be helpful in understanding the effects of manual therapy on spinal motion.

All analysis has been performed at C1-C2 level. Segmental motion components are analyzed on C0-1 and C1-2.

This experimental part of the study includes the methods and materials from studies of Cattrysse et.al (2007); hence the methodological part is identical. The following information is derived from Cattrysse et. al [28].

2.3 Methods and materials

2.3.1 Specimens

Twenty fresh human spinal specimens were included in the study. Nine specimens from male and 11 from female subjects. Each specimen included the occiput, the cervical segments and the first two thoracic vertebrae. The mean age of the specimens was 80 year (±11 years) with a range 59–97. Room temperature was controlled between 15° and 20 °C and humidity was above 60% to prevent dehydration of the specimens during the test procedure.

2.3.2 Instruments

An adapted Zebris CMS20 ultrasound-based motion tracking system (Zebris Medical GmbH – Germany) was used in this study. The accuracy of the system has been studied using a single hinge phantom. One transmitter and the receiver of the device were mounted on a high accuracy rotary stage (Time and Precision Ltd., Baringstoke, England) making it possible to produce angular displacements with an accuracy of 0.02° per step. The standard deviations can be used as an indicative measure of error. An overall deviation of 0.04° occurs on the main axis on a total measurement range of 75° of motion of the phantom. Standard deviations of 0.25° and 0.29° occur on the other axes. Differences between the performed angular displacements and the angles calculated can be partly attributed to cross-talk effects. After applying a correction technique for misalignment between the axis of the phantom and the reference frame defined during the set-up of the Zebris system, based on an optimization technique [28] these standard deviations for the real and the measured angles can be reduced to 0.20 °and 0.13°. The system thus reproduces angles of movements with an accuracy of less than 0.1° for the main motion component and 0.2° for the coupled components.

2.3.3 Methods

In all specimens the skin, subcutaneous tissue and muscles were dissected, leaving the muscular insertions and ligaments intact. This dissection is necessary to prevent limitation of movements and uncontrolled coupled motions that might occur due to the fixation of the ultrasound system on the segments. Moreover, the biomechanical changes within the muscles might alter the results. It has however been demonstrated that the biomechanical properties of the tendons and ligaments do not change due to conservation by freezing [29,30]. Specially fabricated fixation tools were inserted in the parietal part of the occiput, the transverse process of the atlas and the transverse process of the axis. The transmitters and receiver of the Zebris system were mounted on these fixation tools. The optimal positioning of the device was controlled for every specimen prior to the start of the mobilizations. Fixation pins were drilled crosslinked through the corpus of the second thoracic vertebra (T2). The specimen was mounted in a wooden frame by these fixation pins. In this way the specimen was positioned as if the subject was in a supine position on an examination table (fig. 5). The preliminary dissection and the optimal positioning of the fixation tools assured free mobility of the cervical spine trough full range of motion in axial rotation, lateral bending, flexion–extension and combined directions.

Fig 5. Experimental set-up with the specimen in supine position and fixation of the ultrasound system [1]

3D electromagnetic tracking sensors were fixed on the head, C1 and C2. Subsequently, each specimen was first moved in the three main planes of motion. Consequently in all specimens a C1-2 segmental manipulative high velocity thrust with rotation was performed and registrated.
All manipulation techniques were performed three times consecutively by two investigators with several years of experience in manual therapy, in a test-retest situation. The test-retest order was assigned randomly for the two investigators. Investigators were blinded from the analysis data of the system during testing. One of the examiners was familiar with the examined techniques for many years. The other usually performed similar but not identical mobilizing techniques and familiarized with the specific techniques described above before the testing period. Both examiners performed a trial with feedback of the tracking system in a test-retest situation on one specimen to familiarize with the techniques and the test set-up.

2.3.4 3D Angle of movements

The angles of movement used in the present analysis are the angles reproduced from the Zebris-winbiomechanics software. A graphical representation of the calculated angels has been presented by Wang et al. [31]. The definition of the local reference frame used by the Zebris system is based on three markers L, R and F. The point L (left) was chosen on a marker inserted on the left transverse process of the axis, the point R (right) on the right transverse process and the point F (front) centrally on the anterior side of the corpus. Although the International Society of Biomechanics (ISB) provides guidelines defining the local reference frame for mid cervical spinal segments it does not define standards for local reference frames on the atlas, or axis [32]. Due to the nature of the experiment and the specific anatomy of the upper cervical vertebrae the centre of the corpus could not be defined. The above described frames for atlas and axis were therefore defined and the labeling of the axes was chosen in congruency with the ISB guidelines.

The axes are defined as follows:

- Z-axis: from right to left transverse process: segmental flexion–extension axis.
- X-axis: from the anterior centre of the corpus perpendicular to the X-axis: segmental lateral bending axis.
- Y-axis: perpendicular to the X and Y axes: segmental axial rotation axis.

The direction of the Z-axis was reversed to create a right handed orthogonal reference frame. For reasons of clearness of the graphical and numerical representation the sign of the angles around the Y-axis was changed. In this way an axial rotation and a lateral bending to the same side are indicated by the same sign (left and right, respectively, represented by - and +signs) (fig 6).

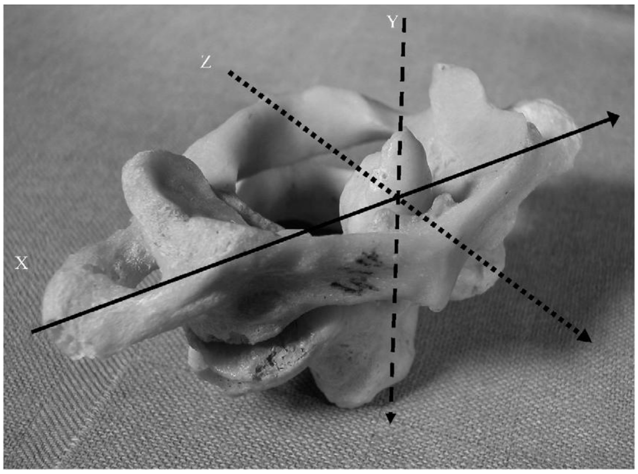

Fig 6. Bone embedded coordinate system on C1: X-axis (segmental lateral bending), Y-axis (segmental axial rotation), Z-axis (segmental flexion-extension) [1]

2.3.5 Analysis of data using Mathcad professional Software

Thrust moment was considered as a derivate in the maximum or minimum of a function wave.

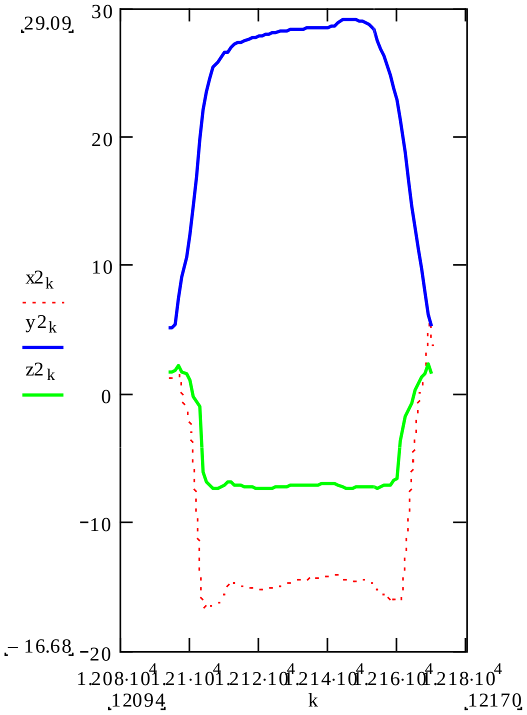

Fig 7. Thrust moment (x, y, z) from dataset in the Mathcad professional Software

In the 3D model x, y, z represent respectively flexion-extension, axial rotation, and lateral bending (fig 7).

The starting and final points of the thrust were identified in all directions (x, y, z) and then these values were considered such as speed (tab 8) and acceleration (tab 9).

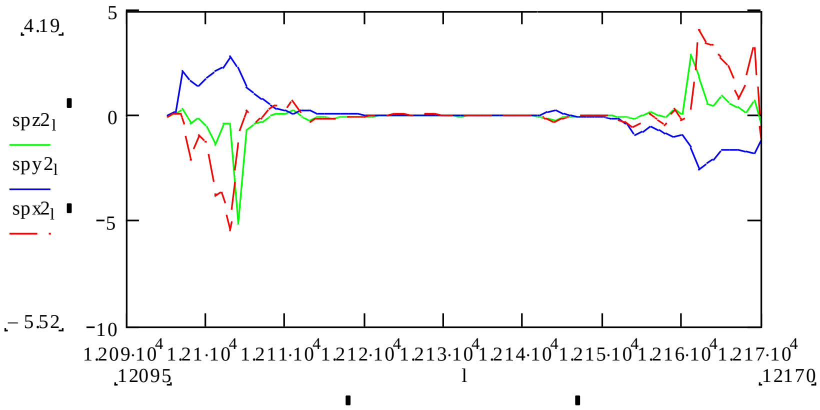

Fig 8. Starting of the analyzing of speed in all directions (x, y, z)

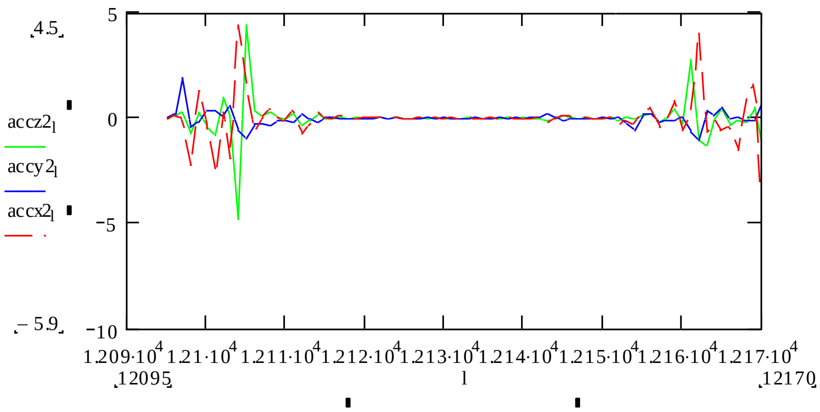

Fig 9. Starting of the analyzing of acceleration in all directions (x, y, z)

Speed as change in position over time and acceleration as change in speed over time were calculated.

These two variables, speed and acceleration, served to distinguish the effect and the contribution of the thrust on the kinematics, especially the speed because it is the rate of change of distance with time (fig 10).

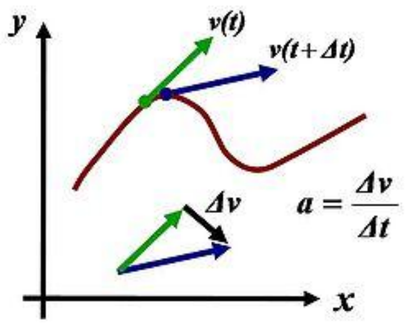

Fig 10. The speed: the rate of change of distance with time

2.3.6 Data validated

In each specimen four tests were considered: test (t) and retest (r) for both therapists. In the analysis of registration with Mathcad professional Software, seven out of eighty tests were not considered in the statistical analysis because there was not a clear thrust. This was due to the fact that there was no presence of the acceleration (0 value): in fact in these cases there was not a maximum or minimum in the wave due to technical error (1 case) or manual technical error (6 cases).

2.3.7 Data Analysis of motion coupling patterns

The patterns of motion coupling between the main axial rotation motion and the coupled lateral bending movement component were analyzed. Five parameters were defined to describe these coupling patterns in an objective way. The range of motion was calculated for the main axial rotation movements as well as the range of motion of the coupled lateral bending and the flexion–extension components.

The cross-correlation between the main axial rotation and the coupled lateral bending was calculated. This cross-correlation parameter can be regarded as the equivalent of a Pearson correlation coefficient.

The ratio between the main axial rotation and the coupled lateral bending was defined as the ratio between the standard deviations of main and coupled motion components and thus depicts the ratio over the whole course of the mobilization.

2.4 Statistical Analysis

Raw data were stored as ASCII files and later processed by Mathcad professional Software using a predefined routine. Then, data were transferred to Excel database.

For all statistical calculations SPSS 14.0, Med Calc and Power and Analysis Software were used.

The Kolmorov-Smirnov goodness of fit test was performed to control the normal distribution of data within these five parameters and descriptive statistics were calculated. The reproducibility of the results was studied by analyzing differences as well as correlations between test and retest results.

The presence of difference between the mean of the three movements (X,Y,Z) in C0-C1 and C1-C2 was analyzed with a non-parametric measure as Wilcoxon test.

The strength of the correlation between parameters in different measurements situations was estimated by the Spearman's correlation. Significance was tested using the 5% rejection level ($p < 0{,}05$).

A Bland-Altman plot was used as graphical method to estimate differences between two techniques plotted against the averages of the two techniques as agreement.

2.5 Results

2.5.1 Power analysis

In each hypothesis a statistical probability of error is associated. The decision to accept or reject the null hypothesis is never completely certain since it is based on a probability.
There are two kinds of errors that can be made in significance testing: (1) a true null hypothesis can be incorrectly rejected and (2) a false null hypothesis can fail to be rejected. The former error is called a Type I error and the latter error is called a Type II error. These two types of errors are defined in the table 1.

Tab 1. Type I and Type II error

Statistical Decision	True State of the Null Hypothesis	
	H_0 True	H_0 False
Reject H_0	Type I error	Correct
Do not Reject H_0	Correct	Type II error

The probability of a Type I error is designated by the Greek letter alpha (a) and is called the Type I error rate; the probability of a Type II error (the Type II error rate) is designated by the Greek letter beta (ß) . A Type II error is only an error in the sense that an opportunity to reject the null hypothesis correctly was lost. It is not an error in the sense that an incorrect conclusion was drawn since no conclusion is drawn when the null hypothesis is not rejected.
The power and the error I were calculated by Power and analysis Software taking the mean from the differences between t1r1t2r2 (in between group differences) and SD from de exact data from t1r1t2r2 (within group SD) for each variable in C2-C1. Descriptive Statistics are presented in table 2.

Tab 2. Descriptive Statistics from C1-C2 in X,Y, Z for each test : t1, r1 t2, r2

	N	Minimum	Maximum	Mean	SD
X12t1	18	,13	2,47	,8806	,66090
X12r1	18	,21	2,05	1,0656	,60343
X12t2	19	,07	2,57	,8589	,75441
X12r2	18	,27	2,52	1,1717	,73574
Y12t1	18	,00	8,52	1,1756	2,07927
Y12r1	18	,00	3,23	1,0167	1,12519
Y12t2	19	,01	3,75	1,4026	1,25838
Y12r2	18	,00	2,31	,7222	,73546
Z12t1	18	,00	7,14	,8606	1,76264
Z12r1	18	,02	5,21	1,1567	1,35996
Z12t2	19	,00	3,48	1,1079	,96201
Z12r2	18	,00	4,06	,8872	1,10234
Valid N (listwise)	14				

The table shows the mean from differences between t1r1t2r2 (in between group differences) and SD from de exact data from t1r1t2r2 (within group SD) for each variable in C2-C1

Legend:
X=flexion-extension
Y=axial rotation
Z=lateral bending
t1=test of the first therapist
r1=retest of the fist therapist
t2=test of the second therapist
r2=retest of the second therapist
SD= standard deviation

In X, Y, Z ROM of C1-C2 was performed a study with 20 pairs of subjects.

The mean and SD for each motion component (ROM) according to predefined axes (X, Y, Z) is reported in the table 3.

Present data indicate that the difference in the response of matched pairs is distributed from 0,65 to 1,26 of mean.

With a true difference in the mean response of matched pairs in a range from 0,67 to 1,24, we will be able to reject the null hypothesis that this response difference is zero with probability (power) within a range from 0.957 to 0.995.
In all ROM (X,Y,Z) the Type I error probability associated with this test of this null hypothesis is 0,05, so we can say that this is a good power analysis.

Tab 3. SD and Mean : mean of differences between t1r1t2r2 (in between group differences) and SD (within group SD)

	X C1-C2	**Y C1-C2**	**Z C1-C2**
SD	1,096083	0,669504	1,243024
Mean	1,263432	0,653833	1,11725

Legend:
X= lateral bending movement
Y=axial rotation movement
Z=flexion-extension movement

2.5.2 The Kolmorov-Smirnov test

Which kind of population are we?

Many statistical tests and procedures are based on specific distributional assumptions. The assumption of normality is particularly common in classical statistical tests. When a population is an expression of random deviation from a central default value (e.g. measurement error) and is composed at least by more than 30 cases, the pattern of its distribution tends to approach the normal distribution. In this way the study of this population may apply characteristics of normal distribution and we can use a parametric test. If the distributional assumption is not justified, using a non-parametric or robust technique may be required.

In this study we have continue values but we have only 20 specimens. The Kolmogorov-Smirnov (KS) test is used to decide if a sample comes from a population with a specific distribution. By non-parametric, we mean a technique that is not based on a specific distributional assumption. By parametric, we mean a statistical technique that performs well under a wide range of distributional assumptions.

The KS statistic quantifies a distance between the empirical distribution function of the sample and the cumulative distribution function of the reference distribution, or between the empirical distribution functions of two samples. The null distribution of this statistic is calculated under the null hypothesis that the samples are drawn from the same distribution (in the two-sample case) or that the sample is drawn from the reference distribution (in the one-sample case). In each case, the distributions considered under the null hypothesis are continuous distributions but are otherwise unrestricted.

We used the two-sample KS, this test is one of the most useful and general nonparametric methods for comparing two samples, as it is sensitive to differences in both location and shape of the empirical cumulative distribution functions of the two samples.

Forty variables were considered: for each specimen there are three directions of movement (X, Y, Z) and two measures of relations (correlation, ratio) in C0-C1 and in C1-C2. As explained above, measurements were performed 4 times (two tests: t1, t2, and two retests r1, r2) so we get 20 variables for C0-C1 and 20 for C1-C2.

The results of the two-sample KS are reported in a table in the addendum 1.

The distribution seems to be approximate to the normal distribution. In fact, only 8 out of 40 variables are statistically significant, 8 variables in the distribution seems to be differ from the normal view, so less than 5% of the differences is random. Since not all results are like a Gaussian distribution, we can use a nonparametric method to explain the statistical analysis.

2.5.3 Reliability analysis: inter and intra examiner

Four consequent manipulations have been performed on each cadaver by two physiotherapists under the same conditions. Manipulations were carried out by the two physiotherapists in a random order. As specimens were mobilized by two different physical therapists for two different times, the reliability of measuring intra-examiner and inter-examiner could be examined with the aim of knowing the reproducibility of kinematics motion coupling parameters during the thrust manipulation in the atlanto-axial joint. In fact, inter-rater reliability is the variation in measurements when taken by different persons but with the same method or instruments. Test-retest reliability is the variation in measurements taken by a single person or instrument on the same item and under the same conditions. This includes intra-rater reliability (addendum 2,3).

Codice campo modificato

Codice campo modificato

Codice campo modificato

In the addendum 3 intra reliability and inter reliability results are presented. Only 7 out of 60 variables are statistically significant, 5 out of 7 significances results refer to inter-examinator comparisons.

So generally this reliability analysis is not significant but it is needed to combine these results with the correlation analysis before trying out conclusions.

Descriptive statistics in X,Y,Z about C1-C2 are reported in the table 4, and those about C1-C0 in the table 5. The relative ranks and statistics tests are in addendum.

Tab 4. Descriptive Statistics X,Y,Z C1-C2

	N	Minimum	Maximum	Mean	Std. Deviation
x12t1	18	,00	8,52	1,1756	2,07927
x12r1	18	,00	3,23	1,0167	1,12519
x12t2	19	,01	3,75	1,4026	1,25838
x12r2	18	,00	2,31	,7222	,73546
y12t1	18	,13	2,47	,8806	,66090
y12r1	18	,21	2,05	1,0656	,60343
y12t2	19	,07	2,57	,8589	,75441
y12r2	18	,27	2,52	1,1717	,73574
z12t1	18	,00	7,14	,8606	1,76264
z12r1	18	,02	5,21	1,1567	1,35996
z12t2	19	,00	3,48	1,1079	,96201
z12r2	18	,00	4,06	,8872	1,10234
CORr12t1	18	-1,00	1,00	-,2777	,85530
CORr12r1	18	-1,00	981,00	54,1482	231,31301
CORr12t2	19	-,99	,98	,2717	,74139
CORr12r2	18	-,99	,97	,2243	,71188
RATIO12t1	18	,29	10,34	2,6460	3,09164
RATIO12r1	18	,21	3,76	1,5501	,98165
RATIO12t2	19	,43	14,42	2,8771	3,28775
RATIO12r2	18	,51	6,99	2,2950	1,72794
Valid N (listwise)	14				

Legend:
X=flexion-extension
Y=axial rotation
Z=lateral bending
t1=test of the first therapist
r1=retest of the fist therapist
t2=test of the second therapist
r2=retest of the second therapist
SD= standard deviation

Tab 5. Descriptive Statistics X,Y,Z C0-C1

	N	Minimum	Maximum	Mean	Std. Deviation
x01t1	18	,00	5,40	1,1561	1,73466
x01r1	18	,00	5,36	1,6156	1,59846
x01t2	19	,00	2,66	,7589	,84094
x01r2	18	,00	2,45	,7061	,74959
y01t1	18	,00	1,25	,4356	,40602
y01r1	18	,00	1,98	,6294	,63061
y01t2	19	,00	1,52	,3032	,40358
y01r2	18	,00	,74	,1839	,22429
z01t1	18	,00	3,51	,5322	1,04044
z01r1	18	,00	1,58	,2911	,40388
z01t2	19	,00	1,65	,3232	,41808
z01r2	18	,00	1,00	,1772	,25699
CORR01t1	18	-,99	,99	,1051	,84166
CORR01r1	18	-,99	1,00	-,0663	,75786
CORR01t2	19	-,90	,99	,2319	,67441
CORR01r2	18	-1,00	1,00	,0381	,75915
RATIO01t1	18	,213	8,388	2,11428	2,101725
RATIO01r1	18	,40	10,14	1,8711	2,42480
RATIO01t2	19	,17	6,99	1,6532	1,67197
RATIO01r2	18	,26	2,55	1,2782	,71084
Valid N (listwise)	14				

Legend:
X=flexion-extension
Y=axial rotation
Z=lateral bending
t1=test of the first therapist
r1=retest of the fist therapist
t2=test of the second therapist
r2=retest of the second therapist
SD= standard deviation

2.5.4 Spearman correlation

We wanted to find out the correlation between two variables and used a bivariate analysis which measures the association's strengths. When two variables vary together, statisticians say that there is covariation or correlation. The correlation coefficient, r, quantifies the direction and magnitude of correlation. Correlation calculations do not discriminate between X and Y, but rather quantify the relationship between the two variables. The value of the correlation coefficient varies between +1 and -1 (tab 6). When the value of the correlation coefficient lies around ± 1, then it is said to be a perfect degree of association between the two variables. As the value goes towards 0, the relationship between the two variables will be weaker.

Tab 6. Interpreting correlation results (coefficient r), SPSS 14.0

Value of r (or rs)	Interpretation
r= 0	The two variables do not vary together at all.
0 > r > 1	The two variables tend to increase or decrease together.
r = 1.0	Perfect correlation.
-1 > r > 0	One variable increases as the other decreases.
r = -1.0	Perfect negative or inverse correlation.

Generally statistic analyses use three types of correlation: Pearson correlation, Kendall rank correlation and Spearman correlation. We used spearman because it returns nonparametric values; in fact Spearman rank correlation test does not assume any assumptions about the distribution. The P value answers this question: If there is really no correlation between two parameters in the overall population, what is the chance that random sampling would result in a correlation coefficient as far from zero (or further) as observed in this experiment?

The results of Spearman correlation are reported in addendum 4. In all manipulations it shows that the correlation is not significant between two variables: the P value is large, the data does not give any reason to conclude that the correlation is real. This does not mean that there is no correlation at all.

We just have not evidence that the correlation is real and not a coincidence, maybe the values are so small that is not possible to discriminate a true correlation.

We can conclude that, generally, the reliability test (with Wilcoxon test) is not significant but no correlation (Spearman) is present. Probably the mean is small and SD is very large: the results from the data are accurate but not precise.

2.5.5 Compare Means

How much movement occurs due to the HVT in C1-C2? How much movement occurs non intentional in C0-C1 with the HVT ?

2.5.5.1 Analysis of differences in means

The Wilcoxon signed Ranks test was performed to answer to those questions.

The Wilcoxon signed-rank test, sometimes called the Wilcoxon matched-pairs test, is also for two dependent samples where the variable of interest is interval. Like the paired or related sample *t*-test, it involves difference's comparisons between measurements, so it requires that the data are measured at an interval level of measurements. However it does not require assumptions about the form of the distribution of the measurements. It should therefore be used whenever the distributional assumptions that underlie the *t*-test cannot be satisfied. However, it is more powerful than the sign test because it takes more information into account. Specifically, the Wilcoxon test factors in the size as well as the sign of the paired differences. It assesses the null hypothesis that the medians of two samples do not differ, or that the median of one sample does not differ from a known value.

The average value between four tests (t1,r1,t2,r2) was taken for each specimen in X,Y,Z. Then the mean of average value in all specimens in each component (X, Y, Z) was calculated. Descriptive statistics about final means in X,Y,Z of this population is well described in the table 7. The ranks and other calculations are reported in addendum 5.

Tab 7. Descriptive Statistics of difference in means in X, Y, Z for C1-C2 and C0-C1

	N	Minimum	Maximum	Mean	Std. Deviation
Xm12	20	,0725	3,4975	1,054833	,8571868
Ym12	20	,0950	2,5375	1,057208	,7233913
Zm12	20	,3150	1,9000	,999542	,5334666
Xm01	20	,0375	,6625	,385083	,1760187
Ym01	20	,1100	2,9433	**,993792**	,7507310
Zm01	20	,0000	1,1700	,344625	,3348986
Valid N (listwise)	20				

Legend:
X=flexion-extension
Y=axial rotation
Z=lateral bending
SD= standard deviation

Which is the main motion component during high velocity thrust?

In C1-C2 any comparisons between 3 dimensional movements within the same segment manipulated is not significant while in C0-C1 p-value in Y-X and Z-Y comparisons is significant with a 0,001 p-value (tab 8).

Tab 8. Test Statistics between means of X,Y,Z within the same level.

	Ym12 - Xm12	Zm12 - Xm12	Zm12 - Ym12	Ym01 - Xm01	Zm01 - Xm01	Zm01 - Ym01
Z	-,448(a)	-,187(b)	-,112(b)	-3,211(a)	-1,008(b)	-3,285(b)
Asymp. Sig. (2-tailed)	,654	,852	,911	**,001**	,313	**,001**

Legend:
a Based on negative ranks.
b Based on positive ranks.
c Wilcoxon Signed Ranks Test

2.5.5.2 Analysis of means in differences

We need to use an average value of four tester for each variable (X,Y,Z) to compare C0-C1 and C1-C2 to analyze relations (tab 9).

Tab 9.Test Statistics: average value (t1, r1, t2,r2) C1-2 against average value (t1,r1,t2,r2) C0-C1

	Xm01 - Xm12	Ym01 - Ym12	Zm01 - Zm12
Z	-2,949(a)	-,597(a)	-3,360(a)
Asymp. Sig. (2-tailed)	**,003**	,550	**,001**

Legend:

a Based on positive ranks.

b Wilcoxon Signed Ranks Test

There are significant differences between C1-C2 and C0-C1 in the mean of X and Z: it finds a same trend of difference (of C1-C2 and C0-C1) in the movement during the thrust. However there is no difference between C1-C2 and C0-C1 in mean of Y. The answer is in the table 7: all mean in C1-C2 are higher than in C0-C1, except the mean of Y in C0-C1 (0,99) which shows an high value as well as all mean in C1-C2. So it’s normal to distinguish differences between X and Z and not in Y: in rotation (Y) high values are present both in C1-C2 than in C0-C1 (tab 7).

2.5.5.3 Interpretations of results

It will be better to read the interpretation of all results with attention to the medium value and it's SD (tab 10), which could be more interesting for this goal.
In C1-C2 the mean between X,Y,Z is similar (0,99-1,05), so there is not a main movement that occurs intentionally during the HVT ($p>0,05$ in all results). Perhaps we would have expected higher value in the mean rotation (Y) in according to previous study of Cattrysse et al [25] but if on the one hand in C1-C2 there are no difference between mean of X,Y,Z , on the other hand the mean rotation (Y) in C0-C1 differs ($p<0,05$) from the mean of flexion-extension (X) and lateral bending (Z), in fact, the Wilcoxon test is significant (tab 11) and the mean of Y in C0-C1 is bigger than other mean in the same level (Y and Z). This means that the manipulation in rotation of C1-C2 involves a simultaneous non intentional rotation (Y) in C0-C1 during the high velocity thrust.
In this way the results seems clear but each conclusion could be confused. In fact, we have to observe carefully the motion coupling pattern (controlateral or ipsilateral) from data collected in mathcad software. So the motion coupling patterns appear to be mixed and it can be concluded there is not a common trend in coupling pattern. Maybe in this way any difference within C1-C2 is difficult to demonstrate. Since we have a small population of specimens and small values with a mixed coupling pattern it is difficult to show differences, so these results can't be consistent to make definitive conclusions.
We can only conclude that there are clear high values of movement in the mean of all movements (X,Y,Z) in C1-C2 (0,99-1,05 range) respect to C0-C1 (0,34-0,99 range) (tab 10). In rotation (Y) high values are evident both in C1-C2 than in C0-C1 anyway, no difference within C1-C2 among X,Y,Z is present, while in C0-C1 the difference of rotation (Y) , in respect to X and Z, is very significant. The manipulation in rotation of C1-C2 involves a simultaneous non intentional rotation (Y) in C0-C1 during the high velocity thrust.

2.5.5.4 Results showed in the Bland-Altman plot

A Bland-Altman plot (difference plot) is used to show results just discussed. Descriptive statistics are reported in the table 10.

Bland and Altman blame the practice of evaluating graphically the correlation between two measurements by the graph of dispersion and proposed a technique more appropriate and easier to use and interpretation: analysis of differences, yb-ya, according to the graphic medium (yb+ya)/2.

This technique is founded on the principle that if measurements are equivalent, the best estimate of the actual size is represented by the arithmetic mean of the two measures.

Moreover, the values reported in the diagram (difference and average measures) are independent.

Therefore, if differences are randomly around the average, the mean difference provides an estimate of the constant component of inaccuracy and the standard error of the measures can be easily derived from the variance of the differences.

Horizontal lines are drawn at the mean difference, and at the limits of agreement, which are defined as the mean difference plus and minus 1.96 times the standard deviation of the differences.

The aim of these plots is to find an agreement among each mean of each variable of C12 and C01 in X (fig 11), Y (fig 12) and Z (fig 13).

Tab 10. Descriptive Statistics about the mean in X,Y,Z in C1-C2 and C0-C1

	N	Minimum	Maximum	Mean	Std. Deviation
meanX12	20	,07	3,50	1,0545	,85752
meanY12	20	,32	1,90	,9994	,53344
meanZ12	20	,08	3,76	1,0475	,90033
meanX01	20	,10	2,54	1,0570	,72391
meanY01	20	,04	,66	,3855	,17626
meanZ01	20	,00	1,17	,3445	,33462
Valid N (listwise)	20				

Legend:
X=flexion-extension
Y=axial rotation
Z=lateral bending
01=C0-C1
12=C1-C2
SD=standard deviation

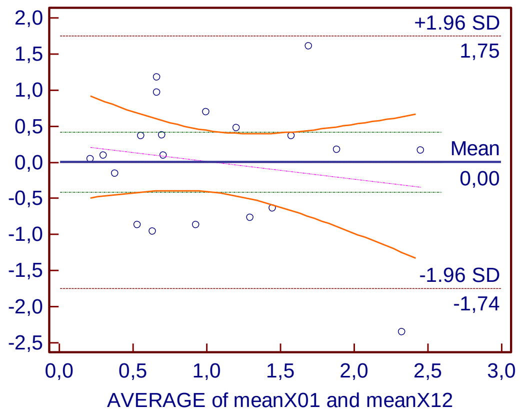

Fig 11. Bland-Altman X12-X01

Legend:
X=flexion-extension
Y=axial rotation
Z=lateral bending
In Y axis= difference between the mean X01-X12
In X axis= average of mean X01 and mean X12

The mean (horizontal line) is perfect (0,00) but the range of SD is a little bit large (+1.75 to 1,74).

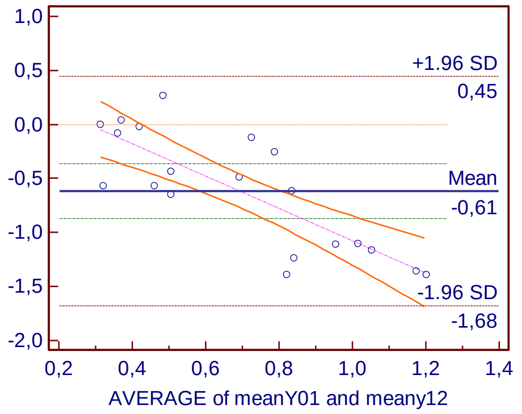

Fig 12. Bland-Altman Y12-Y01

Legend:
X=flexion-extension
Y=axial rotation
Z=lateral bending
In Y axis= difference between the mean X01-X12
In X axis= average of mean X01 and mean X12

The mean (horizontal line) is almost near to the best mean (-0,61) but the SD is too large (+1,96;-1,68).

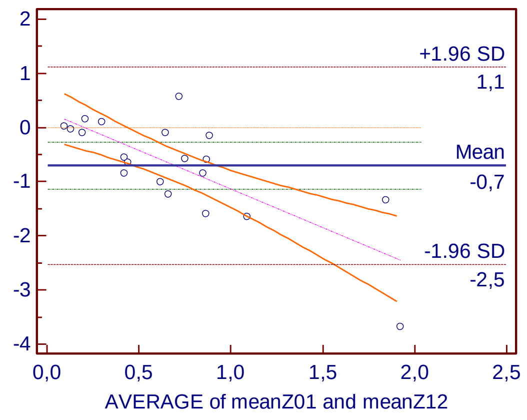

Fig 13.Bland-Altman Z12-Z01

Legend:
X=flexion-extension
Y=axial rotation
Z=lateral bending
In Y axis= difference between the mean X01-X12
In X axis= average of mean X01 and mean X12

The mean (horizontal line) is almost near to the best value (-0,7) but the range of SD is too large (+1.96 to -1,96).

There is a common trend in all plots: the mean is close to zero and no differences are present (mean= 0 is the ideal result).

It means that there is a good agreement between measurements, despite this, the medium range among X,Y,Z of agreement's limits (+1.96 to -1,96) are too large to indicate an acceptable inter- and intra-observer reproducibility.

2.6 Discussion

A 3D kinematic analysis of fresh human spinal specimens in a test-retest situation with two observations is presented in this study.

The purpose is to compare the results derived from the use of a ZEBRIS ultrasound-based coordinate measuring system during high velocity thrust manipulation in C2-C1 level to present the quality and quantity analysis of movement. Natalis and Konig found an overall accuracy for angular rotations of 0.6° for the Zebris system [33]. The results of the validation procedure of the Zebris CMS20 device used in this study are in agreement with the analysis of segmental motions during manual mobilization. The Zebris-winbiomechanics software calculates 3D motion angles in a specific way which is different from the classical Euler/Cardan angles approach or the projection Method [28].

Observing the results of the intra- and inter-observer comparison, an insufficient level of reproducibility for all therapists is present related to correlations not significant.

According to Cattrysse et. al [28] there seems to be a general tendency towards higher intra-observer reliability compared to inter-observer results in segmental manual mobilization[1,28,34]. It is not well known whether the experience of the therapist/examiner may play a role in the intra-examiner reproducibility. Although some authors report no influence from experience [35] other studies indicate a possible positive influence of experience [36]. Moreover, in the previous work, inter-observer data revealed an insufficient level of reproducibility for all three techniques performed [28] for most of the analyzed parameters.

These results have to be interpreted in view of the limitations inherent to the present possibilities for analyzing 3D kinematics of manual induced motion of the atlanto-axial joint.

The reliability analysis calculated in this work by Wilcoxon test and Spearman correlation was inconsistent. The mean of population is small and SD is too large to indicate an acceptable inter- and intra-observer reproducibility. So, the results from the data are accurate but not precise.

The aim of this thesis intended to analyze what is the main component of the movement during the thrust. Wilcoxon test was calculated to show differences, but the results were not significant. Spearman test was calculated to show correlations but there were no agreements. These results are somewhat different from what we would have expected because different results are published in the previous work of Cattrysse et. al (2006) [25] about seven embalmed human cadavers in an *in vitro* registration of UC segmental coupled motions during HVT. The methodological part was nearly identical. The results showed that all planar induced movements include 3-dimensional coupled motions. During the main flexion extension motion on the atlanto-occipital segment important associated rotation and lateral bending takes place that can even equal or sometimes exceed the main motion. The rotational HVT on the level C1-C2 results in an additional axial rotation component of approximately 2°, with almost no rotational components in flexion-extension or lateral bending directions (fig 14).

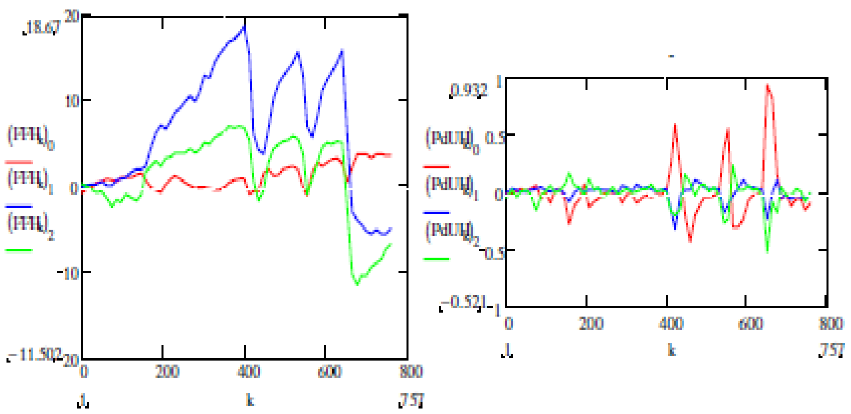

Fig 14. Cumulative finite helical angles C1-C2 during rotational HVT 3D arthrokinematic analysis of coupled motion in the human upper cervical-spine: in vitro analysis of high velocity thrust techniques [33].

Legend:
Blu line=axial rotation
Green line= lateral bending
Red line= flexion-extension

In the present study the results are different (fig 15): the rotational HVT on the level C1-C2 results just in an additional axial rotation component of approximately 1,06° with a consistent presence of flexion-extension (1,05°) and lateral banding (0,99°) (fig 16). The rotation HVT in C1-C2 induces an additional axial rotation in C0-C1 of 0,99°, which has higher value than flexion-extension (0,38°) and lateral bending (0,34°) (fig 17).

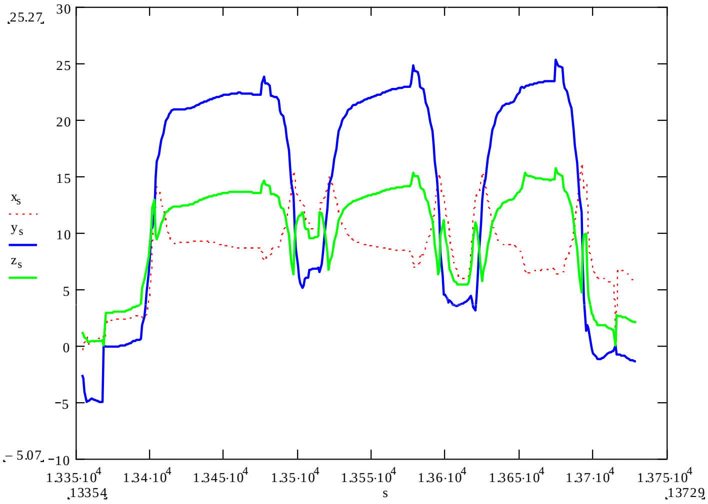

Fig 15. Angles and motion components in according to the Zebris software during rotational HVT in C1-C2 (specimen num 182)

Legend:
Blu line=axial rotation
Green line= lateral bending
Red line= flexion-extension

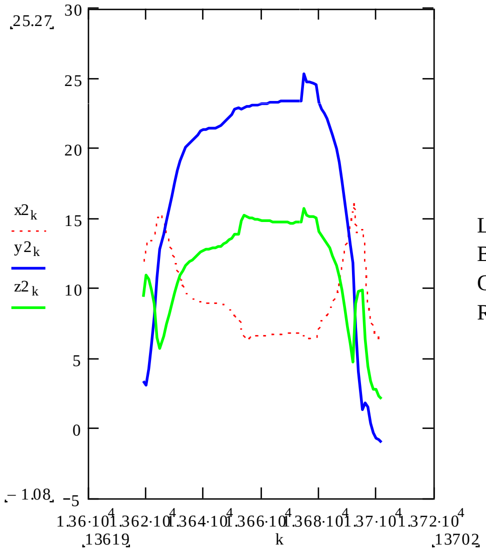

Legend:
Blu line=axial rotation
Green line= lateral bending
Red line= flexion-extension

Fig 16. Starting of the thrust: Angles in C1-C2 during High velocity Thrust according to the Zebris software during rotational HVT in C1-C2 (specimen num 182)

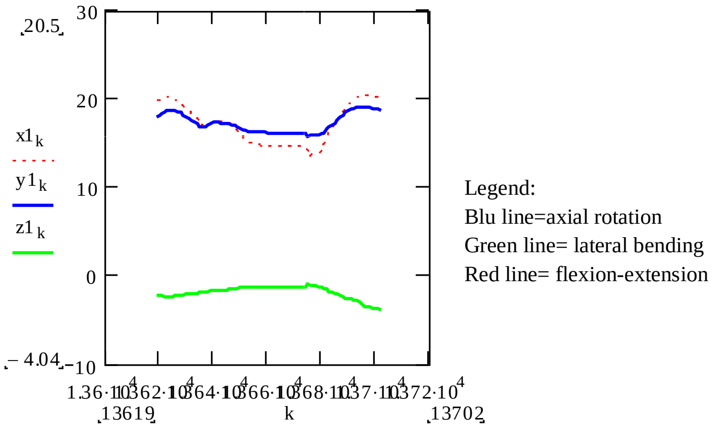

Fig 17. Starting of the thrust: angles in C0-C1 during High velocity Thrust according to the Zebris software during rotational HVT in C1-C2 (specimen num 182)

The largest motion at the atlanto-occipital level is flexion-extension as is described in literature while at the atlanto-axial level the rotation is the motion whit the largest amplitude [19]. Maybe the reason of difference between both studies can be explained by the following points.

The previous work [25] used results and graphic representations from FHA, instead of angles of movement used in this study as presented by Wang et al [31]. In fact, the Zebris-winbiomechanics software calculates 3D-motion angles in a specific way which is different from the classical Euler/Cardan angles approach or the projection method. A mathematical reconstruction based on the spherical geometry of the angles calculated by Zebris-system [1] is presented in addendum 6. It has been demonstrated that different approaches may led to different angular representation of 3D-motion [14].

Another aspect that can explain the diversity being the difference between embalmed and un-embalmed material: strangely enough one would expect to have larger motion components in the un-embalmed as tissue are softer but maybe there is an effect on reaching the pre-manipulative positions.

Then, the numerical representation of the population in both studies (embalmed and un-embalmed) is different: twenty specimen in this study and seven in the previous study. Moreover, in the previous study on HVT [25] there was no analysis of reproducibility. The specimens were analysed once by one observer.

2.7 Conclusion

Previously a power analysis was performed: high power (0.957-0,995) and alpha error = 0.05 (xC1-C2, yC1-C2, zC1-C2) were found in the way to be more sure of the following tests.

KS test was applied: since not all results are like a Gaussian distribution, we used a nonparametric methods to explain the statistical analysis and describe its interpretation.

The results indicate inconsistent analysis reliability related to the not significant test of Spearman’s correlation. Maybe we have a small mean with the large SD: the results from the data are accurate but not precise.

These results have to be interpreted in view of the limitations inherent to the present possibilities for analyzing 3D kinematics of manual induced motion of the atlanto-axial joint.

During HVT we could not find what is the major movement that occurs. Surely, there are clear high values in all movements (X,Y,Z) in C1-C2 (0,99-1,05 range) respect to C0-C1 (0,34-0,99 range). In rotation (Y) high values are evident both in C1-C2 than in C0-C1 as explained in the mean. Anyway, no difference among X,Y,Z in C1-C2 is present, while in C0-C1 the difference of rotation (Y), respect to X and Z, is very significant ($p<0,05$). The manipulation in rotation of C1-C2 involves a simultaneous non intentional rotation (Y) in C0-C1 during the high velocity thrust.

While in the previous study [25] the rotational HVT on the level C1-C2 results in an additional axial rotation component of approximately 2°, with almost no rotational components in flexion-extension or lateral bending directions, in this thesis rotational HVT on the level C1-C2 shows just in an additional axial rotation component of approximately 1,06° with a consistent presence of flexion-extension (1,05°) and lateral banding (0,99°). The difference can be answered in several reasons of protocol: embalmed and un-embalmed specimens, number of specimens, graphical representations, reliability analysis.

The previous work [25] didn’t look at C0-C1 level during HVT. In this study the rotation HVT in C1-C2 induces an additional axial rotation in C0-C1 of 0,99°, which has higher value than flexion-extension (0,38°) and lateral bending (0,34°).

The results of this in vitro study suggest that it might be important in a therapy situation to choose specific techniques according to the desired effect [37,38]. *In vivo* studies will have to confirm this hypothesis.

The results may also be relevant to further *in vivo* research of motion coupling patterns in the upper cervical spine. More work must be carried out in order to better analyze HVT techniques in the upper-cervical spines.

Addenda

Addendum 1: Kolmogorov-Smirnov Test

One-Sample Kolmogorov-Smirnov Test

		x12t1	y12t1	z12t1	CORr12t1	RATIO12t1	x01t1	y01t1	z01t1
N		18	18	18	18	18	18	18	18
Normal Parameters[a,b]	Mean	1,1756	,8806	,8606	-,2777	2,6460	1,1561	,4356	,5322
	Std. Deviation	2,07927	,66090	1,76264	,85530	3,09164	1,73466	,40602	1,04044
Most Extreme Differences	Absolute	,331	,142	,336	,311	,357	,350	,211	,340
	Positive	,331	,142	,336	,311	,357	,350	,211	,340
	Negative	-,286	-,128	-,313	-,200	-,223	-,253	-,142	-,304
Kolmogorov-Smirnov Z		1,405	,604	1,426	1,320	1,515	1,486	,894	1,443
Asymp. Sig. (2-tailed)		,038	,859	,034	,061	,020	,024	,401	,031

		CORR01t1	RATIO01t1	x12r1	y12r1	z12r1	CORr12r1	RATIO1212	x01r1
N		18	18	18	18	18	18	18	18
Normal Parameters[a,b]	Mean	,1051	2,11428	1,0167	1,0656	1,1567	54,1482	1,5501	1,6156
	Std. Deviation	,84166	2,101725	1,12519	,60343	1,35996	231,31301	,98165	1,59846
Most Extreme Differences	Absolute	,238	,259	,226	,121	,202	,535	,112	,182
	Positive	,207	,259	,226	,112	,183	,535	,112	,182
	Negative	-,238	-,183	-,183	-,121	-,202	-,406	-,086	-,156
Kolmogorov-Smirnov Z		1,011	1,097	,960	,515	,855	2,271	,475	,771
Asymp. Sig. (2-tailed)		,259	,180	,316	,953	,457	,000	,978	,592

		y01r1	z01r1	CORR01r1	RATIO01r1	x12t2	y12t2	z12t2
N		18	18	18	18	19	19	19
Normal Parameters[a,b]	Mean	,6294	,2911	-,0663	1,8711	1,4026	,8589	1,1079
	Std. Deviation	,63061	,40388	,75786	2,42480	1,25838	,75441	,96201
Most Extreme Differences	Absolute	,181	,236	,178	,362	,139	,205	,154
	Positive	,181	,201	,178	,362	,139	,205	,154
	Negative	-,159	-,236	-,142	-,273	-,134	-,148	-,125
Kolmogorov-Smirnov Z		,769	,999	,753	1,536	,606	,892	,671
Asymp. Sig. (2-tailed)		,596	,271	,621	,018	,856	,404	,759

a. Test distribution is Normal.

b. Calculated from data.

The Kolmogorov-Smirnov Test compares an observed cumulative distribution function to a theoretical cumulative distribution.

<u>Addendum 2</u>: Ranks Wilcoxon test

X C1-C2 Ranks		N	Mean Rank	Sum of Ranks
x12r1 - x12t1	Negative Ranks	7(a)	7,64	53,50
	Positive Ranks	8(b)	8,31	66,50
	Ties	1(c)		
	Total	16		
x12r2 - x12t2	Negative Ranks	12(d)	11,17	134,00
	Positive Ranks	6(e)	6,17	37,00
	Ties	0(f)		
	Total	18		
x12t2 - x12t1	Negative Ranks	6(g)	8,00	48,00
	Positive Ranks	10(h)	8,80	88,00
	Ties	1(i)		
	Total	17		
x12r2 - x12r1	Negative Ranks	11(j)	9,09	100,00
	Positive Ranks	5(k)	7,20	36,00
	Ties	0(l)		
	Total	16		
x12r2 - x12t1	Negative Ranks	9(m)	9,78	88,00
	Positive Ranks	7(n)	6,86	48,00
	Ties	0(o)		
	Total	16		
x12t2 - x12r1	Negative Ranks	9(p)	7,00	63,00
	Positive Ranks	8(q)	11,25	90,00
	Ties	0(r)		
	Total	17		

a x12r1 < x12t1
b x12r1 > x12t1
c x12r1 = x12t1
d x12r2 < x12t2
e x12r2 > x12t2
f x12r2 = x12t2
g x12t2 < x12t1
h x12t2 > x12t1
i x12t2 = x12t1
j x12r2 < x12r1
k x12r2 > x12r1
l x12r2 = x12r1
m x12r2 < x12t1
n x12r2 > x12t1
o x12r2 = x12t1
p x12t2 < x12r1
q x12t2 > x12r1
r x12t2 = x12r1

Y C1-C2 Ranks		N	Mean Rank	Sum of Ranks
y12r1 - y12t1	Negative Ranks	6(a)	7,00	42,00
	Positive Ranks	10(b)	9,40	94,00
	Ties	0(c)		
	Total	16		
y12r2 - y12t2	Negative Ranks	7(d)	8,29	58,00
	Positive Ranks	11(e)	10,27	113,00
	Ties	0(f)		
	Total	18		
y12t2 - y12t1	Negative Ranks	7(g)	8,07	56,50
	Positive Ranks	10(h)	9,65	96,50
	Ties	0(i)		
	Total	17		
y12r2 - y12r1	Negative Ranks	6(j)	8,42	50,50
	Positive Ranks	10(k)	8,55	85,50
	Ties	0(l)		
	Total	16		
y12r2 - y12t1	Negative Ranks	7(m)	7,64	53,50
	Positive Ranks	9(n)	9,17	82,50
	Ties	0(o)		
	Total	16		
y12t2 - y12r1	Negative Ranks	10(p)	9,30	93,00
	Positive Ranks	7(q)	8,57	60,00
	Ties	0(r)		
	Total	17		

a y12r1 < y12t1
b y12r1 > y12t1
c y12r1 = y12t1
d y12r2 < y12t2
e y12r2 > y12t2
f y12r2 = y12t2
g y12t2 < y12t1
h y12t2 > y12t1
i y12t2 = y12t1
j y12r2 < y12r1
k y12r2 > y12r1
l y12r2 = y12r1
m y12r2 < y12t1
n y12r2 > y12t1
o y12r2 = y12t1
p y12t2 < y12r1
q y12t2 > y12r1
r y12t2 = y12r1

Z C1-C2 Ranks		N	Mean Rank	Sum of Ranks
z12r1 - z12t1	Negative Ranks	5(a)	5,20	26,00
	Positive Ranks	11(b)	10,00	110,00
	Ties	0(c)		
	Total	16		
z12r2 - z12t2	Negative Ranks	11(d)	11,05	121,50
	Positive Ranks	7(e)	7,07	49,50
	Ties	0(f)		
	Total	18		
z12t2 - z12t1	Negative Ranks	5(g)	6,50	32,50
	Positive Ranks	11(h)	9,41	103,50
	Ties	1(i)		
	Total	17		
z12r2 - z12r1	Negative Ranks	11(j)	8,36	92,00
	Positive Ranks	5(k)	8,80	44,00
	Ties	0(l)		
	Total	16		
z12r2 - z12t1	Negative Ranks	8(m)	8,31	66,50
	Positive Ranks	8(n)	8,69	69,50
	Ties	0(o)		
	Total	16		
z12t2 - z12r1	Negative Ranks	8(p)	9,50	76,00
	Positive Ranks	9(q)	8,56	77,00
	Ties	0(r)		
	Total	17		

a z12r1 < z12t1
b z12r1 > z12t1
c z12r1 = z12t1
d z12r2 < z12t2
e z12r2 > z12t2
f z12r2 = z12t2
g z12t2 < z12t1
h z12t2 > z12t1
i z12t2 = z12t1
j z12r2 < z12r1
k z12r2 > z12r1
l z12r2 = z12r1
m z12r2 < z12t1
n z12r2 > z12t1
o z12r2 = z12t1
p z12t2 < z12r1
q z12t2 > z12r1
r z12t2 = z12r1

Corr C1-C2 Ranks		N	Mean Rank	Sum of Ranks
CORr12r1 - CORr12t1	Negative Ranks	9(a)	7,33	66,00
	Positive Ranks	7(b)	10,00	70,00
	Ties	0(c)		
	Total	16		
CORr12r2 - CORr12t2	Negative Ranks	11(d)	7,82	86,00
	Positive Ranks	6(e)	11,17	67,00
	Ties	1(f)		
	Total	18		
CORr12t2 - CORr12t1	Negative Ranks	6(g)	6,17	37,00
	Positive Ranks	11(h)	10,55	116,00
	Ties	0(i)		
	Total	17		
CORr12r2 - CORr12r1	Negative Ranks	7(j)	6,29	44,00
	Positive Ranks	9(k)	10,22	92,00
	Ties	0(l)		
	Total	16		
CORr12r2 - CORr12t1	Negative Ranks	4(m)	7,25	29,00
	Positive Ranks	12(n)	8,92	107,00
	Ties	0(o)		
	Total	16		
CORr12t2 - CORr12r1	Negative Ranks	5(p)	7,20	36,00
	Positive Ranks	12(q)	9,75	117,00
	Ties	0(r)		
	Total	17		

a CORr12r1 < CORr12t1
b CORr12r1 > CORr12t1
c CORr12r1 = CORr12t1
d CORr12r2 < CORr12t2
e CORr12r2 > CORr12t2
f CORr12r2 = CORr12t2
g CORr12t2 < CORr12t1
h CORr12t2 > CORr12t1
i CORr12t2 = CORr12t1
j CORr12r2 < CORr12r1
k CORr12r2 > CORr12r1
l CORr12r2 = CORr12r1
m CORr12r2 < CORr12t1
n CORr12r2 > CORr12t1
o CORr12r2 = CORr12t1
p CORr12t2 < CORr12r1
q CORr12t2 > CORr12r1
r CORr12t2 = CORr12r1

Ratio C1-C2 Ranks		N	Mean Rank	Sum of Ranks
RATIO12r1 - RATIO12t1	Negative Ranks	9(a)	9,89	89,00
	Positive Ranks	7(b)	6,71	47,00
	Ties	0(c)		
	Total	16		
RATIO12r2 - RATIO12t2	Negative Ranks	10(d)	7,40	74,00
	Positive Ranks	7(e)	11,29	79,00
	Ties	1(f)		
	Total	18		
RATIO12t2 - RATIO12t1	Negative Ranks	7(g)	9,43	66,00
	Positive Ranks	10(h)	8,70	87,00
	Ties	0(i)		
	Total	17		
RATIO12r2 - RATIO12r1	Negative Ranks	4(j)	6,50	26,00
	Positive Ranks	12(k)	9,17	110,00
	Ties	0(l)		
	Total	16		
RATIO12r2 - RATIO12t1	Negative Ranks	8(m)	9,13	73,00
	Positive Ranks	8(n)	7,88	63,00
	Ties	0(o)		
	Total	16		
RATIO12t2 - RATIO12r1	Negative Ranks	5(p)	8,60	43,00
	Positive Ranks	12(q)	9,17	110,00
	Ties	0(r)		
	Total	17		

a RATIO12r1 < RATIO12t1
b RATIO12r1 > RATIO12t1
c RATIO12r1 = RATIO12t1
d RATIO12r2 < RATIO12t2
e RATIO12r2 > RATIO12t2
f RATIO12r2 = RATIO12t2
g RATIO12t2 < RATIO12t1
h RATIO12t2 > RATIO12t1
i RATIO12t2 = RATIO12t1
j RATIO12r2 < RATIO12r1
k RATIO12r2 > RATIO12r1
l RATIO12r2 = RATIO12r1
m RATIO12r2 < RATIO12t1
n RATIO12r2 > RATIO12t1
o RATIO12r2 = RATIO12t1
p RATIO12t2 < RATIO12r1
q RATIO12t2 > RATIO12r1
r RATIO12t2 = RATIO12r1

X C0-C1 Ranks		N	Mean Rank	Sum of Ranks
x01r1 - x01t1	Negative Ranks	5(a)	9,00	45,00
	Positive Ranks	11(b)	8,27	91,00
	Ties	0(c)		
	Total	16		
x01r2 - x01t2	Negative Ranks	8(d)	10,50	84,00
	Positive Ranks	10(e)	8,70	87,00
	Ties	0(f)		
	Total	18		
x01t2 - x01t1	Negative Ranks	8(g)	9,63	77,00
	Positive Ranks	9(h)	8,44	76,00
	Ties	0(i)		
	Total	17		
x01r2 - x01r1	Negative Ranks	11(j)	8,64	95,00
	Positive Ranks	4(k)	6,25	25,00
	Ties	1(l)		
	Total	16		
x01r2 - x01t1	Negative Ranks	8(m)	10,00	80,00
	Positive Ranks	8(n)	7,00	56,00
	Ties	0(o)		
	Total	16		
x01t2 - x01r1	Negative Ranks	9(p)	11,33	102,00
	Positive Ranks	8(q)	6,38	51,00
	Ties	0(r)		
	Total	17		

a x01r1 < x01t1
b x01r1 > x01t1
c x01r1 = x01t1
d x01r2 < x01t2
e x01r2 > x01t2
f x01r2 = x01t2
g x01t2 < x01t1
h x01t2 > x01t1
i x01t2 = x01t1
j x01r2 < x01r1
k x01r2 > x01r1
l x01r2 = x01r1
m x01r2 < x01t1
n x01r2 > x01t1
o x01r2 = x01t1
p x01t2 < x01r1
q x01t2 > x01r1
r x01t2 = x01r1

Y C0-C1	Ranks	N	Mean Rank	Sum of Ranks
y01r1 - y01t1	Negative Ranks	9(a)	6,17	55,50
	Positive Ranks	7(b)	11,50	80,50
	Ties	0(c)		
	Total	16		
y01r2 - y01t2	Negative Ranks	8(d)	8,94	71,50
	Positive Ranks	7(e)	6,93	48,50
	Ties	3(f)		
	Total	18		
y01t2 - y01t1	Negative Ranks	10(g)	10,25	102,50
	Positive Ranks	7(h)	7,21	50,50
	Ties	0(i)		
	Total	17		
y01r2 - y01r1	Negative Ranks	10(j)	8,95	89,50
	Positive Ranks	5(k)	6,10	30,50
	Ties	1(l)		
	Total	16		
y01r2 - y01t1	Negative Ranks	13(m)	9,19	119,50
	Positive Ranks	3(n)	5,50	16,50
	Ties	0(o)		
	Total	16		
y01t2 - y01r1	Negative Ranks	9(p)	11,17	100,50
	Positive Ranks	8(q)	6,56	52,50
	Ties	0(r)		
	Total	17		

a y01r1 < y01t1
b y01r1 > y01t1
c y01r1 = y01t1
d y01r2 < y01t2
e y01r2 > y01t2
f y01r2 = y01t2
g y01t2 < y01t1
h y01t2 > y01t1
i y01t2 = y01t1
j y01r2 < y01r1
k y01r2 > y01r1
l y01r2 = y01r1
m y01r2 < y01t1
n y01r2 > y01t1
o y01r2 = y01t1
p y01t2 < y01r1
q y01t2 > y01r1
r y01t2 = y01r1

Z C0-C1	Ranks	N	Mean Rank	Sum of Ranks
z01r1 - z01t1	Negative Ranks	7(a)	9,71	68,00
	Positive Ranks	9(b)	7,56	68,00
	Ties	0(c)		
	Total	16		
z01r2 - z01t2	Negative Ranks	11(d)	9,00	99,00
	Positive Ranks	5(e)	7,40	37,00
	Ties	2(f)		
	Total	18		
z01t2 - z01t1	Negative Ranks	8(g)	10,13	81,00
	Positive Ranks	9(h)	8,00	72,00
	Ties	0(i)		
	Total	17		
z01r2 - z01r1	Negative Ranks	6(j)	9,58	57,50
	Positive Ranks	8(k)	5,94	47,50
	Ties	2(l)		
	Total	16		
z01r2 - z01t1	Negative Ranks	10(m)	8,95	89,50
	Positive Ranks	6(n)	7,75	46,50
	Ties	0(o)		
	Total	16		
z01t2 - z01r1	Negative Ranks	5(p)	8,90	44,50
	Positive Ranks	11(q)	8,32	91,50
	Ties	1(r)		
	Total	17		

a z01r1 < z01t1
b z01r1 > z01t1
c z01r1 = z01t1
d z01r2 < z01t2
e z01r2 > z01t2
f z01r2 = z01t2
g z01t2 < z01t1
h z01t2 > z01t1
i z01t2 = z01t1
j z01r2 < z01r1
k z01r2 > z01r1
l z01r2 = z01r1
m z01r2 < z01t1
n z01r2 > z01t1
o z01r2 = z01t1
p z01t2 < z01r1
q z01t2 > z01r1
r z01t2 = z01r1

Corr C0-C1 **Ranks**		N	Mean Rank	Sum of Ranks
CORR01r1 - CORR01t1	Negative Ranks	12(a)	8,75	105,00
	Positive Ranks	4(b)	7,75	31,00
	Ties	0(c)		
	Total	16		
CORR01r2 - CORR01t2	Negative Ranks	9(d)	10,89	98,00
	Positive Ranks	9(e)	8,11	73,00
	Ties	0(f)		
	Total	18		
CORR01t2 - CORR01t1	Negative Ranks	8(g)	8,88	71,00
	Positive Ranks	9(h)	9,11	82,00
	Ties	0(i)		
	Total	17		
CORR01r2 - CORR01r1	Negative Ranks	8(j)	7,88	63,00
	Positive Ranks	8(k)	9,13	73,00
	Ties	0(l)		
	Total	16		
CORR01r2 - CORR01t1	Negative Ranks	10(m)	9,80	98,00
	Positive Ranks	6(n)	6,33	38,00
	Ties	0(o)		
	Total	16		
CORR01t2 - CORR01r1	Negative Ranks	7(p)	9,00	63,00
	Positive Ranks	10(q)	9,00	90,00
	Ties	0(r)		
	Total	17		

a CORR01r1 < CORR01t1
b CORR01r1 > CORR01t1
c CORR01r1 = CORR01t1
d CORR01r2 < CORR01t2
e CORR01r2 > CORR01t2
f CORR01r2 = CORR01t2
g CORR01t2 < CORR01t1
h CORR01t2 > CORR01t1
i CORR01t2 = CORR01t1
j CORR01r2 < CORR01r1
k CORR01r2 > CORR01r1
l CORR01r2 = CORR01r1
m CORR01r2 < CORR01t1
n CORR01r2 > CORR01t1
o CORR01r2 = CORR01t1
p CORR01t2 < CORR01r1
q CORR01t2 > CORR01r1
r CORR01t2 = CORR01r1

Ratio C0-C1 Ranks		N	Mean Rank	Sum of Ranks
RATIO01r1 - RATIO01t1	Negative Ranks	11(a)	8,09	89,00
	Positive Ranks	5(b)	9,40	47,00
	Ties	0(c)		
	Total	16		
RATIO01r2 - RATIO01t2	Negative Ranks	9(d)	11,00	99,00
	Positive Ranks	9(e)	8,00	72,00
	Ties	0(f)		
	Total	18		
RATIO01t2 - RATIO01t1	Negative Ranks	10(g)	9,90	99,00
	Positive Ranks	7(h)	7,71	54,00
	Ties	0(i)		
	Total	17		
RATIO01r2 - RATIO01r1	Negative Ranks	6(j)	8,50	51,00
	Positive Ranks	9(k)	7,67	69,00
	Ties	1(l)		
	Total	16		
RATIO01r2 - RATIO01t1	Negative Ranks	8(m)	10,50	84,00
	Positive Ranks	8(n)	6,50	52,00
	Ties	0(o)		
	Total	16		
RATIO01t2 - RATIO01r1	Negative Ranks	9(p)	8,56	77,00
	Positive Ranks	8(q)	9,50	76,00
	Ties	0(r)		
	Total	17		

a RATIO01r1 < RATIO01t1
b RATIO01r1 > RATIO01t1
c RATIO01r1 = RATIO01t1
d RATIO01r2 < RATIO01t2
e RATIO01r2 > RATIO01t2
f RATIO01r2 = RATIO01t2
g RATIO01t2 < RATIO01t1
h RATIO01t2 > RATIO01t1
i RATIO01t2 = RATIO01t1
j RATIO01r2 < RATIO01r1
k RATIO01r2 > RATIO01r1
l RATIO01r2 = RATIO01r1
m RATIO01r2 < RATIO01t1
n RATIO01r2 > RATIO01t1
o RATIO01r2 = RATIO01t1
p RATIO01t2 < RATIO01r1
q RATIO01t2 > RATIO01r1
r RATIO01t2 = RATIO01r1

Addendum 3: Test Statistics in reliability analysis

Tab ad3-1: X , flession-extension C1-C2

Test Statistics[c,d]

			x12r1 - x12t1	x12r2 - x12t2	x12t2 - x12t1	x12r2 - x12r1	x12r2 - x12t1	x12t2 - x12r1
Z			-,369[a]	-2,113[b]	-1,034[a]	-1,655[b]	-1,034[b]	-,639[a]
Asymp. Sig. (2-tailed)			,712	,035	,301	,098	,301	,523
Monte Carlo Sig. (2-tailed)	Sig.		,850	,000	,350	,100	,350	,600
	95% Confidence Interval	Lower Bound	,694	,000	,141	,000	,141	,385
		Upper Bound	1,000	,139	,559	,231	,559	,815
Monte Carlo Sig. (1-tailed)	Sig.		,350	,000	,100	,050	,250	,150
	95% Confidence Interval	Lower Bound	,141	,000	,000	,000	,060	,000
		Upper Bound	,559	,139	,231	,146	,440	,306

a. Based on negative ranks.

b. Based on positive ranks.

c. Wilcoxon Signed Ranks Test

d. Based on 20 sampled tables with starting seed 334431365.

The Sig. in r2-t2 is reported in the Bland Altman plot

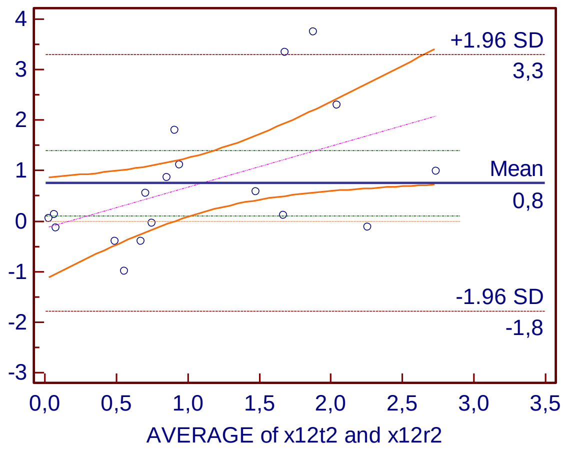

Fig ad3-1: axial rotation r2-t2 C1-C2 in the Bland Altman plot

Tab ad3-2: Y, Axial rotation C1-C2

Test Statistics[c,d]

			y12r1 - y12t1	y12r2 - y12t2	y12t2 - y12t1	y12r2 - y12r1	y12r2 - y12t1	y12t2 - y12r1
Z			-1,344[a]	-1,198[a]	-,947[a]	-,905[a]	-,750[a]	-,781[b]
Asymp. Sig. (2-tailed)			,179	,231	,344	,365	,453	,435
Monte Carlo Sig. (2-tailed)	Sig.		,150	,150	,350	,450	,600	,350
	95% Confidence Interval	Lower Bound	,000	,000	,141	,232	,385	,141
		Upper Bound	,306	,306	,559	,668	,815	,559
Monte Carlo Sig. (1-tailed)	Sig.		,100	,100	,200	,200	,250	,100
	95% Confidence Interval	Lower Bound	,000	,000	,025	,025	,060	,000
		Upper Bound	,231	,231	,375	,375	,440	,231

a. Based on negative ranks.

b. Based on positive ranks.

c. Wilcoxon Signed Ranks Test

d. Based on 20 sampled tables with starting seed 2000000.

Tab ad3-3: Z, Lateral bending C1-C2

Test Statistics[c,d]

			z12r1 - z12t1	z12r2 - z12t2	z12t2 - z12t1	z12r2 - z12r1	z12r2 - z12t1	z12t2 - z12r1
Z			-2,174[a]	-1,568[b]	-1,836[a]	-1,241[b]	-,078[a]	-,024[a]
Asymp. Sig. (2-tailed)			,030	,117	,066	,215	,938	,981
Monte Carlo Sig. (2-tailed)	Sig.		,150	,150	,200	,400	1,000	1,000
	95% Confidence Interval	Lower Bound	,000	,000	,025	,185	,861	,861
		Upper Bound	,306	,306	,375	,615	1,000	1,000
Monte Carlo Sig. (1-tailed)	Sig.		,050	,150	,050	,300	,300	,300
	95% Confidence Interval	Lower Bound	,000	,000	,000	,099	,099	,099
		Upper Bound	,146	,306	,146	,501	,501	,501

a. Based on negative ranks.

b. Based on positive ranks.

c. Wilcoxon Signed Ranks Test

d. Based on 20 sampled tables with starting seed 1502173562.

The Sig. in t1-r1 is reported in the Bland Altman plot

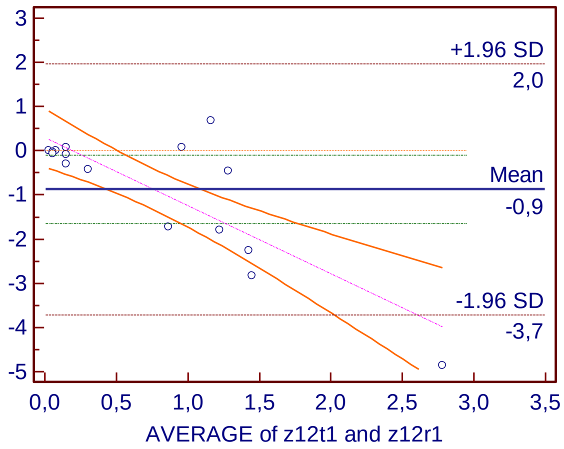

Fig ad3-3:lateral bending t1-r1 C1-C2 in the Bland Altman plot

Tab ad3-4: Correlazione in C1-C2

Test Statistics[c,d]

			CORr12r1 - CORr12t1	CORr12r2 - CORr12t2	CORr12t2 - CORr12t1	CORr12r2 - CORr12r1	CORr12r2 - CORr12t1	CORr12t2 - CORr12r1
Z			-,103[a]	-,450[b]	-1,870[a]	-1,241[a]	-2,017[a]	-1,917[a]
Asymp. Sig. (2-tailed)			,918	,653	,062	,215	,044	,055
Monte Carlo Sig. (2-tailed)	Sig.		1,000	,900	,050	,250	,050	,050
	95% Confidence Interval	Lower Bound	,861	,769	,000	,060	,000	,000
		Upper Bound	1,000	1,000	,146	,440	,146	,146
Monte Carlo Sig. (1-tailed)	Sig.		,400	,450	,000	,100	,000	,000
	95% Confidence Interval	Lower Bound	,185	,232	,000	,000	,000	,000
		Upper Bound	,615	,668	,139	,231	,139	,139

a. Based on negative ranks.

b. Based on positive ranks.

c. Wilcoxon Signed Ranks Test

d. Based on 20 sampled tables with starting seed 92208573.

The Sig. in t1-t2 and r2-t1 is reported in the Bland Altman plot

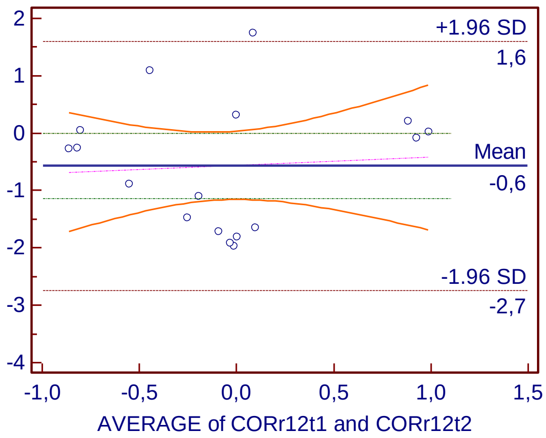

Fig ad3-4a: t1-t2 C1-C2 in the Bland Altman plot

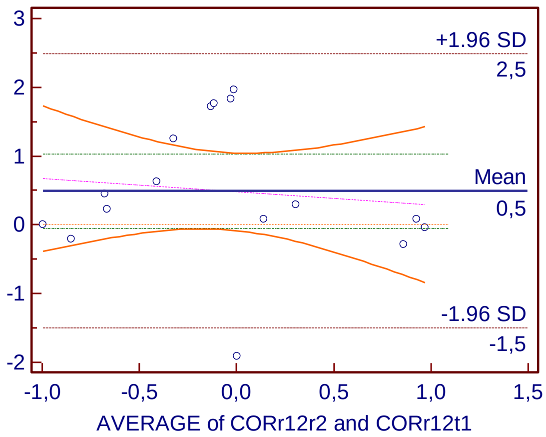

Fig ad3-4b: Correlation r1-t1 C1-C2 in the Bland Altman plot

Tab ad3-5: Ratio in C1-C2

Test Statistics[c,d]

			RATIO12r1 - RATIO12t1	RATIO12r2 - RATIO12t2	RATIO12t2 - RATIO12t1	RATIO12r2 - RATIO12r1	RATIO12r2 - RATIO12t1	RATIO12t2 - CORr12r1
Z			-1,086[a]	-,118[b]	-,497[b]	-2,172[b]	-,259[a]	-2,817[b]
Asymp. Sig. (2-tailed)			,278	,906	,619	,030	,796	,005
Monte Carlo Sig. (2-tailed)	Sig.		,300	,900	,650	,050	,850	,000
	95% Confidence Interval	Lower Bound	,099	,769	,441	,000	,694	,000
		Upper Bound	,501	1,000	,859	,146	1,000	,139
Monte Carlo Sig. (1-tailed)	Sig.		,150	,350	,250	,000	,350	,000
	95% Confidence Interval	Lower Bound	,000	,141	,060	,000	,141	,000
		Upper Bound	,306	,559	,440	,139	,559	,139

a. Based on positive ranks.

b. Based on negative ranks.

c. Wilcoxon Signed Ranks Test

d. Based on 20 sampled tables with starting seed 562334227.

The Sig. in r1-r2 is reported in the Bland Altman plot

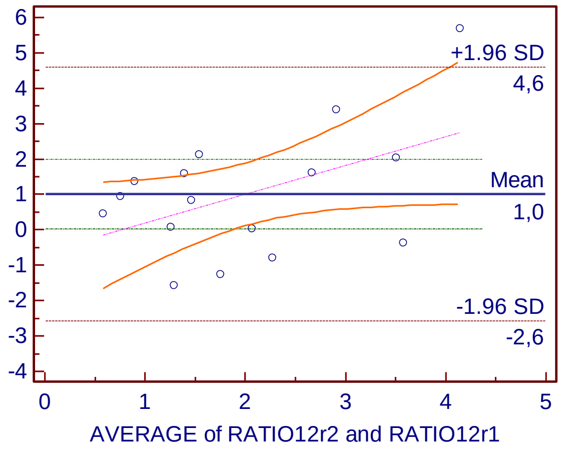

Fig ad3-5: r1-r2C1-C2 in the Bland Altman plot

Tab ad3-6: X, Flession-extension in C0-C1

Test Statistics[c,d]

			x01r1 - x01t1	x01r2 - x01t2	x01t2 - x01t1	x01r2 - x01r1	x01r2 - x01t1	x01t2 - x01r1
Z			-1,189[a]	-,065[a]	-,024[b]	-1,988[b]	-,621[b]	-1,207[b]
Asymp. Sig. (2-tailed)			,234	,948	,981	,047	,535	,227
Monte Carlo Sig. (2-tailed)	Sig.		,250	,900	1,000	,000	,550	,350
	95% Confidence Interval	Lower Bound	,060	,769	,861	,000	,332	,141
		Upper Bound	,440	1,000	1,000	,139	,768	,559
Monte Carlo Sig. (1-tailed)	Sig.		,100	,450	,500	,000	,250	,150
	95% Confidence Interval	Lower Bound	,000	,232	,281	,000	,060	,000
		Upper Bound	,231	,668	,719	,139	,440	,306

a. Based on negative ranks.

b. Based on positive ranks.

c. Wilcoxon Signed Ranks Test

d. Based on 20 sampled tables with starting seed 475497203.

The Sig. in r1-r2 is reported in the Bland Altman plot

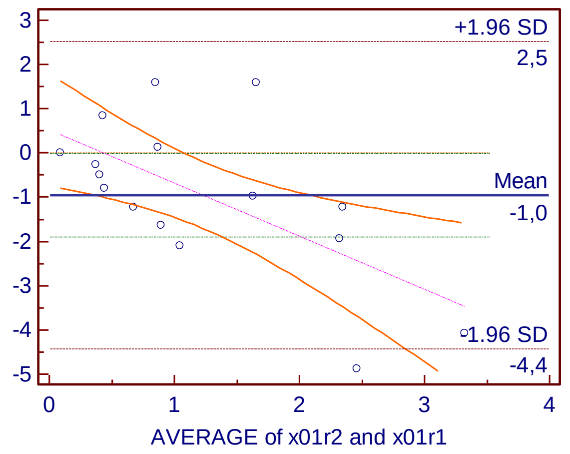

Fig ad3-6: flexion -extension r2-r1 C0-C1 in the bland Altman plot

Tab ad3-7: Y, Axial rotation in C0-C1

Test Statistics[c,d]

			y01r1 - y01t1	y01r2 - y01t2	y01t2 - y01t1	y01r2 - y01r1	y01r2 - y01t1	y01t2 - y01r1
Z			-,647[a]	-,653[b]	-1,231[b]	-1,676[b]	-2,664[b]	-1,136[b]
Asymp. Sig. (2-tailed)			,518	,514	,218	,094	,008	,256
Monte Carlo Sig. (2-tailed)	Sig.		,400	,350	,200	,000	,050	,200
	95% Confidence Interval	Lower Bound	,185	,141	,025	,000	,000	,025
		Upper Bound	,615	,559	,375	,139	,146	,375
Monte Carlo Sig. (1-tailed)	Sig.		,150	,200	,100	,000	,000	,100
	95% Confidence Interval	Lower Bound	,000	,025	,000	,000	,000	,000
		Upper Bound	,306	,375	,231	,139	,139	,231

a. Based on negative ranks.

b. Based on positive ranks.

c. Wilcoxon Signed Ranks Test

d. Based on 20 sampled tables with starting seed 1585587178.

The Sig. in r1-r2 and in r2-t1 is reported in the Bland Altman plot

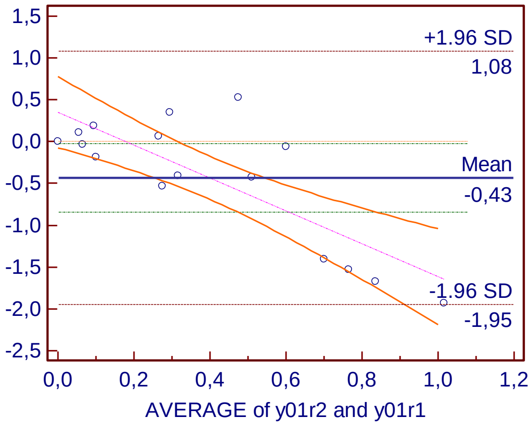

Fig ad3-7a:axial rotation r1-r2 C0-C1 in the Bland Altman plot

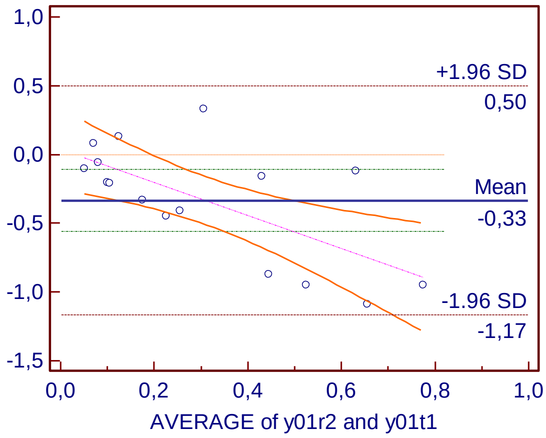

Fig ad3-7b:axial rotation t1-r2 C0-C1 in the Bland Altman plot

Tab ad3-8: Y, Lateral bending in C0-C1

Test Statistics[d,e]

			z01r1 - z01t1	z01r2 - z01t2	z01t2 - z01t1	z01r2 - z01r1	z01r2 - z01t1	z01t2 - z01r1
Z			,000[a]	-1,603[b]	-,213[b]	-,314[b]	-1,112[b]	-1,215[c]
Asymp. Sig. (2-tailed)			1,000	,109	,831	,753	,266	,224
Monte Carlo Sig. (2-tailed)	Sig.		1,000	,100	,850	,750	,200	,150
	95% Confidence Interval	Lower Bound	,861	,000	,694	,560	,025	,000
		Upper Bound	1,000	,231	1,000	,940	,375	,306
Monte Carlo Sig. (1-tailed)	Sig.		,400	,000	,500	,350	,100	,050
	95% Confidence Interval	Lower Bound	,185	,000	,281	,141	,000	,000
		Upper Bound	,615	,139	,719	,559	,231	,146

a. The sum of negative ranks equals the sum of positive ranks.

b. Based on positive ranks.

c. Based on negative ranks.

d. Wilcoxon Signed Ranks Test

e. Based on 20 sampled tables with starting seed 1487459085.

Tab ad3-9: Correlation in C0-C1

Test Statistics[c,d]

			CORR01r1 - CORR01t1	CORR01r2 - CORR01t2	CORR01t2 - CORR01t1	CORR01r2 - CORR01r1	CORR01r2 - CORR01t1	CORR01t2 - CORR01r1
Z			-1,913[a]	-,544[a]	-,260[b]	-,259[b]	-1,551[a]	-,639[b]
Asymp. Sig. (2-tailed)			,056	,586	,795	,796	,121	,523
Monte Carlo Sig. (2-tailed)	Sig.		,100	,850	,950	,850	,100	,800
	95% Confidence Interval	Lower Bound	,000	,694	,854	,694	,000	,625
		Upper Bound	,231	1,000	1,000	1,000	,231	,975
Monte Carlo Sig. (1-tailed)	Sig.		,050	,350	,500	,450	,050	,500
	95% Confidence Interval	Lower Bound	,000	,141	,281	,232	,000	,281
		Upper Bound	,146	,559	,719	,668	,146	,719

a. Based on positive ranks.

b. Based on negative ranks.

c. Wilcoxon Signed Ranks Test

d. Based on 20 sampled tables with starting seed 1660843777.

Tab ad 3-10:Ratio in C0-C1

Test Statistics[c,d]

			RATIO01r1 - RATIO01t1	RATIO01r2 - RATIO01t2	RATIO01t2 - RATIO01t1	RATIO01r2 - RATIO01r1	RATIO01r2 - RATIO01t1	RATIO01t2 - RATIO01r1
Z			-1,086[a]	-,588[a]	-1,065[a]	-,511[b]	-,827[a]	-,024[a]
Asymp. Sig. (2-tailed)			,278	,557	,287	,609	,408	,981
Monte Carlo Sig. (2-tailed)	Sig.		,400	,900	,350	,850	,650	1,000
	95% Confidence Interval	Lower Bound	,185	,769	,141	,694	,441	,861
		Upper Bound	,615	1,000	,559	1,000	,859	1,000
Monte Carlo Sig. (1-tailed)	Sig.		,150	,350	,150	,400	,350	,400
	95% Confidence Interval	Lower Bound	,000	,141	,000	,185	,141	,185
		Upper Bound	,306	,559	,306	,615	,559	,615

a. Based on positive ranks.

b. Based on negative ranks.

c. Wilcoxon Signed Ranks Test

d. Based on 20 sampled tables with starting seed 1122541128.

Addendum 4: Spearman correlation

Correlations

			x12t1	x01t1	x12r1	x01r1	x12t2	x01t2	x12r2	x01r2
Spearman's rho	x12t1	Correlation Coefficient	1,000	,602**	,141	,324	,088	,091	,279	-,206
		Sig. (2-tailed)	.	,008	,602	,222	,736	,729	,295	,444
		N	18	18	16	16	17	17	16	16
	x01t1	Correlation Coefficient	,602**	1,000	,144	,411	-,121	,128	,159	-,268
		Sig. (2-tailed)	,008	.	,594	,114	,643	,626	,557	,316
		N	18	18	16	16	17	17	16	16
	x12r1	Correlation Coefficient	,141	,144	1,000	,235	,130	,161	,343	-,022
		Sig. (2-tailed)	,602	,594	.	,347	,619	,538	,193	,935
		N	16	16	18	18	17	17	16	16
	x01r1	Correlation Coefficient	,324	,411	,235	1,000	,069	-,201	,397	,009
		Sig. (2-tailed)	,222	,114	,347	.	,794	,439	,128	,974
		N	16	16	18	18	17	17	16	16
	x12t2	Correlation Coefficient	,088	-,121	,130	,069	1,000	-,028	,196	-,412
		Sig. (2-tailed)	,736	,643	,619	,794	.	,909	,437	,090
		N	17	17	17	17	19	19	18	18
	x01t2	Correlation Coefficient	,091	,128	,161	-,201	-,028	1,000	,278	,067
		Sig. (2-tailed)	,729	,626	,538	,439	,909	.	,263	,791
		N	17	17	17	17	19	19	18	18
	x12r2	Correlation Coefficient	,279	,159	,343	,397	,196	,278	1,000	-,123
		Sig. (2-tailed)	,295	,557	,193	,128	,437	,263	.	,626
		N	16	16	16	16	18	18	18	18
	x01r2	Correlation Coefficient	-,206	-,268	-,022	,009	-,412	,067	-,123	1,000
		Sig. (2-tailed)	,444	,316	,935	,974	,090	,791	,626	.
		N	16	16	16	16	18	18	18	18

**. Correlation is significant at the 0.01 level (2-tailed).

<u>Addendum 5</u>:Compare means

Analysis of differences in means

Ranks

		N	Mean Rank	Sum of Ranks
Ym12 - Xm12	Negative Ranks	7(a)	13,29	93,00
	Positive Ranks	13(b)	9,00	117,00
	Ties	0(c)		
	Total	20		
Zm12 - Xm12	Negative Ranks	10(d)	11,00	110,00
	Positive Ranks	10(e)	10,00	100,00
	Ties	0(f)		
	Total	20		
Zm12 - Ym12	Negative Ranks	11(g)	9,82	108,00
	Positive Ranks	9(h)	11,33	102,00
	Ties	0(i)		
	Total	20		
Ym01 - Xm01	Negative Ranks	5(j)	3,80	19,00
	Positive Ranks	15(k)	12,73	191,00
	Ties	0(l)		
	Total	20		
Zm01 - Xm01	Negative Ranks	11(m)	12,00	132,00
	Positive Ranks	9(n)	8,67	78,00
	Ties	0(o)		
	Total	20		
Zm01 - Ym01	Negative Ranks	17(p)	11,35	193,00
	Positive Ranks	3(q)	5,67	17,00
	Ties	0(r)		
	Total	20		

a Ym12 < Xm12
b Ym12 > Xm12
c Ym12 = Xm12
d Zm12 < Xm12
e Zm12 > Xm12
f Zm12 = Xm12
g Zm12 < Ym12
h Zm12 > Ym12
i Zm12 = Ym12
j Ym01 < Xm01
k Ym01 > Xm01
l Ym01 = Xm01
m Zm01 < Xm01
n Zm01 > Xm01
o Zm01 = Xm01

p Zm01 < Ym01
q Zm01 > Ym01
r Zm01 = Ym01

Tab ad5-1: Analysis of differences in means

Test Statistics[c,d]

			Ym12 - Xm12	Zm12 - Ym12	Zm12 - Xm12	Ym01 - Xm01	Zm01 - Ym01	Zm01 - Xm01
Z			-,448[a]	-,112[b]	-,187[b]	-3,211[a]	-3,285[b]	-1,008[b]
Asymp. Sig. (2-tailed)			,654	,911	,852	,001	,001	,313
Monte Carlo Sig. (2-tailed)	Sig.		,650	,950	,850	,000	,000	,300
	95% Confidence Interval	Lower Bound	,441	,854	,694	,000	,000	,099
		Upper Bound	,859	1,000	1,000	,139	,139	,501
Monte Carlo Sig. (1-tailed)	Sig.		,300	,550	,450	,000	,000	,150
	95% Confidence Interval	Lower Bound	,099	,332	,232	,000	,000	,000
		Upper Bound	,501	,768	,668	,139	,139	,306

a. Based on negative ranks.

b. Based on positive ranks.

c. Wilcoxon Signed Ranks Test

d. Based on 20 sampled tables with starting seed 1149983241.

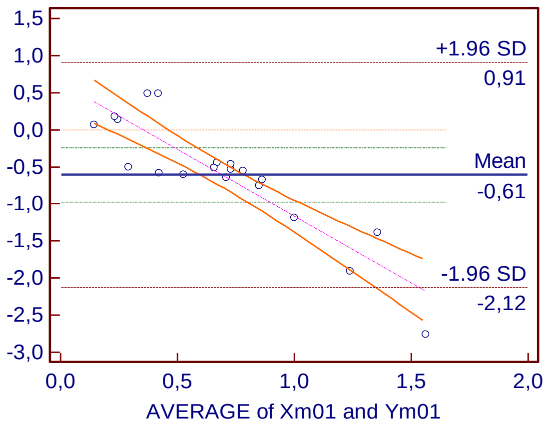

Fig ad5-1a. Bland Altman plot in X-Y C0-C1

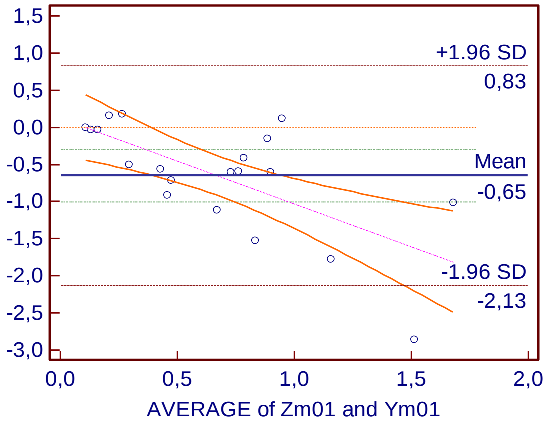

Fig ad5-1b. Bland Altman plot in Z-Y C0-C1

Addendum 6:

mathematical reconstruction based on the spherical geometry of the angles presented by Zebris-winbiomechanics software

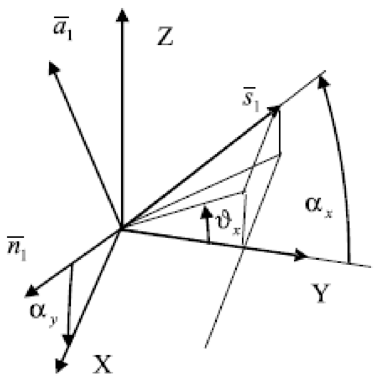

Fig. ad6-1 : angles α_x and ϑ_x

The analytical expression for the angle α_x thus is:

$$\tan(\alpha_x) = \frac{s_z}{a_z}$$

The analytical expression for the angle α_y (as can be deduced from Fig. ad6-1) is:

$$\sin(\alpha_y) = -n_z \quad (1)$$

To determine the angle ϑ_x for the X-axis following the procedure of Zebris, according to Wang et all [31], the local frame $\bar{n}, \bar{s}, \bar{a}$ is rotated first around the Z-axis of the reference frame by the angle $-\alpha_z$ to obtain a frame $\bar{n}_1, \bar{s}_1, \bar{a}_1$.

As this rotation compensates the original rotation around the Z-axis, Fig. ad6-1 does not show the frame $\bar{n}, \bar{s}, \bar{a}$ but only shows the frame $\bar{n}_1, \bar{s}_1, \bar{a}_1$. Next the unit vector $\bar{s}_1$ along the Y-axis of this local frame $\bar{n}_1, \bar{s}_1, \bar{a}_1$ is rotated by the amount ϑ_x around the X-axis of the reference frame, till the vector $\bar{s}_1$ is in the XY plane. The analytical expression for the angle ϑ_x can be calculated with the components of the direction cosines of the unit vectors of the local frame $\bar{n}, \bar{s}, \bar{a}$ along the Z-axis [1].

$$\tan(\vartheta_x) = \frac{s_z}{a_z}\sqrt{1 - n_z^2}$$

As follows from expression (1), the angle ϑ_x practically coincides with the angle ax measured around the local axis with unit vector $\vec{n}_1$ when the direction cosine n_z is small, as can be seen in Fig. ad6. This is the case when the angle α_y is small. The graphical representation in [31] corresponds to the situation where α_y = 0.

Bibliography

1. Cattrysse E., 3D-Analysis of segmental coupled motion during Manual Upper Cervical Spine Mobilization, thesis subitted for the degree of doctor in Rehabilitation Sciences and Physiotherapy, 2007.
2. Gross AR, Kay T, Hondras M, Goldsmith C., Haines T, Peloso P,Kennedy C, Hoving J. Manual therapy for mechanical neck disorders: a systematic review. Manual therapy 2002;7:131-49
3. Klein P, Broers C, Feipel V, Salvia P, Van Geyt B, Dugailly PM, Rooze M.Global 3D head-trunk kinematics during cervical spine manipulation at different levels. Clin Biomech (Bristol, Avon). 2003;18(9):827-31.
4. Cattrysse E, Baeyens JP, Kool P, Clarys JP, Van Roy P. In vitro 3D-Arthrokinematic analysis of Axial rotation and Lateral bending mobilization of the Upper Cervical Spine; Analysis of coupled motions by cross-correlation, ratio and phase-shift characteristics. 9th international conference on 3D-human movement analysis. Valenciennes-France, 2006.
5. Pierre-Michel Dugailly, Stéphane Sobczak,Victor Sholukha, Serge Van Sint Jan, Patrick Salvia,Véronique Feipel, Marcel Rooze. In vitro 3D-kinematics of the upper cervical spine: helical axis and simulation for axial rotation and flexion extension. Surg Radiol Anat. 2010 Feb;32(2):141-51. Epub 2009 Sep 12.
6. Nikolai Bogduk, Susan Mercer, Biomechanics of the cervical spine. I: Normal kinematics Clinical Biomechanics 15 (2000); 633±648.
7. Clare J.Roche, Susan J.King, Peter H Dangerfield, Helen M Carty. The atlanto-axial joint: physiological range of rotation on MRI and CT. Clinical radiology 2002; 57, 103-108.
8. Jull G. Use of high and low velocity cervical manipulative therapy procedures by Australian manipulative physiotherapists. Aust J Physiother 2002;48:189–93.
9. Koes BW, Bouter LM, van Mameren H, Essers AH, Verstegen GM, Hofhuizen DM, et al. Randomised clinical trial of manipulative therapy

and physiotherapy for persistent back and neck complaints: results of one year follow up. BMJ 1992;304:601–5.

10. Gross AR, Hoving JL, Haines TA, Goldsmith CH, Kay T, Aker P, et al. A Cochrane review of manipulation and mobilization for mechanical neck disorders. Spine 2004;29(14):1541–8.
11. Philip S. Bolton, Brian S. Budgell Spinal manipulation and spinal mobilization influence different axial sensory beds, Medical Hypotheses 2006; 66, 258–262
12. Suzanne J. Snodgrass, MMedSc,a Darren A. Rivett, PhD,b and Val J. Robertson, PhDc, manual force applied during cervical mobilization
13. Maitland GD, Banks K, English K, Hengeveld E. Maitland's vertebral manipulation. 7th ed. Oxford7 Butterworth-Heinemann; 2005.
14. Baeyens J. P.; Cattrysse E.; Van Roy P.; Clarys J. P. Measurement of three-dimensional intra-articular kinematics: methodological and interpretation problems. Department of Experimental Anatomy, Vrije Universiteit Brussel, Brussels, Belgium, Ergonomics 2005, 48: 11, 1638-1644
15. Chad Cook, PhD, PT, MBA,a Eric Hegedus, PT, DPT,b Christopher Showalter, PT,c and Phillip S. Sizer Jr, PhD, PTd, Coupling behavior of cervical spine: a systematic review of literature. J Manipulative Physiol Ther 2006;29:570-575
16. Pearcy M, Tibrewal M. Axial rotation and lateral bending in the normal lumbar spine measured by three-dimensional radiography. Spine 1984;9:582-7.
17. Panjabi MM, Summers DJ, Pelker RR, Videman T, Friedlaender GE, Southwick Wo. 3-Dimensional Load-Displacemnt Curves Due to Forces on the Cervical-Spine. Journal of Orthopaedic research 1986;4:152-61
18. Milne N. Composite motion in cervical Disc Segments. Clinical Biomechanics 1993;8:193-202
19. Panjabi MM, Oda T, Crisco JJ, Dvorak J, Grob D. Posture affects motion coupling Patterns of the Upper Cervical-Spine. Journal of Orthopaedic Research 1993;11:525-36

20. Cattrysse E, Baeyens JP, Kool P, Clarys JP and Van Roy P. Does manual mobilization influence motion coupling patterns in the atlanto-axial joint? Journal of Electromyography and Kinesiology 18 (2008) 838–848
21. Triano J, Schultz AB. Motions of the head and torax during neck manipulation. Journal of manipulative and physiological therapeutics. 1994; 17 (9), 573-583.
22. David W. Evans, BSc (Hons) Osta. Mechanisms and effects of spinal high-velocity, low-amplitude thrust manipulation: previous theories. Journal of Manipulative and Physiological Therapeutics 2004; volume 25 number 4, 241-262.
23. Triano J, Schultz AB. Loads transmitted during lumbo-sacral spinal. manipulative therapy. Spine 1997;22(17):1955–64.
24. W. A. Hing, D. A. Reid, M. Monaghanw Manipulation of the cervical spine. Manual Therapy 2003; 8(1), 2–9
25. Cattrysse Erik, Baeyens Jean-Pierre, Clarys Jan-Pieter, Van Roy Peter. Dep. Experimental Anatomy, Vrije Universiteit Brussel, Brussels, Belgium. 3D Arthrokinematic analysis of coupled motion in the human upper-cervical spine:in vitro analysis of high velocity thrust techniques. ISB XXth Congress - ASB 29th Annual Meeting. July 31 - August 5, Cleveland, Ohio
26. Jim M.W. Ngan, Daniel H.K. Chow, Andrew D. Holmes. The kinematics and intra- and inter-therapist consistencies of lower cervical rotational manipulation. Medical Engineering & Physics 27 (2005); 395–401
27. Raquel Martınez-Segura, PT, DO,a Ce´sar Ferna´ndez-de-las-Pen˜as, PT,b Mariana Ruiz-Sa´ez, PT, CO, Cristina Lo´ pez-Jime´nez, PT, DO,d and Cleofa´s Rodrı´guez-Blanco, PT, DO. Immediate Effects on Pain and Range of Motion of Spinal Manipulation. Journal of Manipulative and Physiological Therapeutics Mart´ınez-Segura et al Volume 29, Number 7
28. Cattrysse E., Provyn , Kool P., Gagey O., Clarys J.P., Van Roy P. Reproducibility of kinematic motion coupling parameters during manual upper cervical axial rotation mobilization: A 3-dimensional in vitro study of the atlanto-axial joint. Journal of Electromyography and Kinesiology 19 (2009) 93–104

29. Wilke HJ, Krishchak S, Claes LE. Formalin fixation strongly influences biomechanical properties of the spine. Journal of biomechanics 1996;29:1629-31
30. Panjabi MM, Krag M, Summers D, Videman T. Biomechanical time-tolerence of fresh cadaveric human spine specimens. Journal of Orthopaedic Research 1985;3:292-300.
31. Wang SF, Teng CC, Lin CH. Measurement of cervical range of motion pattern during cyclic neck movement by an ultrasound-based motion system. Manual therapy 10 (2005) 68-72
32. WU GE, Sorin Siegler, Paul Allard, Chris Kirtey, Alberto Leardini, Dieter Rosenbaum, Mike Whittle, Darrly D D'Lima, Luca Cristoforini, Hartmut Witte, Oskar Schmid and Ian Stokes. ISB recommendation on definitions of joint coordinate system of various joints for the reporting of the human joint motion-part I: ankle, hip, and spine. Journal of Biomechanics 2002; Vol.35, num 4, pp. 543-548
33. Natalis M, Konig A. Noninvasive, accurate and reliable measurement of the cervical spine motion with a 3D real-time ultrasound motion analyser. Ultraschall Med 1999;20(2):70–3.
34. Billis EV, Foster NE, Wright CC. Reproducibility and repeatability: errors of three groups of physiotherapists in locating spinal levels by palpation. Manual Ther 2003;8(4):223–32
35. Hawk C, Phongphua C, Bleecker J, Swank L, Lopez D, Rubley T. Preliminary study of the reliability of assessment procedures for indications for chiropractic adjustments of the lumbar spine. J Manip Physiol Ther 1999;22(6):382–9.
36. Cattrysse E, Swinkels RAHM, Oostendorp RAB, Duquet W. Uppercervical instability: are clinical tests reliable? Manual Ther 1997;2(2):91–7.
37. Cattrysse E, Baeyens JP, Clarys JP and Van Roy P. Manual fixation versus locking during upper cervical segmental mobilization. Part 1: An in vitro three-dimensional arthrokinematic analysis of manual flexion-extension mobilization of the atlanto-occipital joint. Manual Therapy 2007;12 (4): 342-52

38. Cattrysse E, Baeyens JP, Clarys JP and Van Roy P. Manual fixation versus locking during upper cervical segmental mobilization. Part 2: An in vitro three-dimensional arthrokinematic analysis of manual axial rotation and lateral bending mobilization of the atlanto-axial joint Manual Therapy 2007; 12 (4): 353-362